Neuronal IL-17 controls *C. elegans* developmental diapause through CEP-1/p53

Abhishiktha Godthi[1,2,], Sehee Min[1,2,], Srijit Das[1], Johnny Cruz-Corchado[1,2], Andrew Deonarine[1], Kara Misel-Wuchter [3], Priya D. Issuree [3] and Veena Prahlad[1,2] *

Affiliations: [1]Department of Cell Stress Biology
Roswell Park - Comprehensive Cancer Center
Elm and Carlton Streets
CGP-BLSC L3-307
Buffalo, New York 14263

[2]Department of Biology,
338 Biology Building East,
143 Biology Building, Iowa City, IA 52242-1324.

[3]Department of Internal Medicine,
503 Eckstein Medical Research Building,
431 Newton Road, Iowa City, IA 52242

***** Corresponding author name: Veena Prahlad

Corresponding author email**:** veena.prahlad@roswellpark.org

Author Contributions

All authors designed the study, performed experiments, analyzed data, and drafted the manuscript. P.D.I coordinated the mammalian experiments; V.P. coordinated *C. elegans* experiments and the project. All authors approved the final version of the manuscript.

Declaration of Interests

The authors declare no competing interests.

Classification

Biological Sciences; Developmental Biology

Keywords:

***C. elegans* p53/ CEP-1, dauer, IL-17, development, immunometabolomic, nutrient signaling.**

This PDF file includes:

Main Text
Figures 1 to 6

Supporting Information:
Extended Methods
Supplementary Figure S1-S14 including Extended Text 1-4
Supplementary Datasets S1 to S14.

Significance. Development in a metazoan requires that the division and differentiation of diverse cells be coordinated with nutrient availability. We show that one mechanism by which this occurs in *C. elegans* is through signaling by the neuronal IL-17 cytokine, ILC-17.1, and its control over p53/CEP-1. In the presence of food, ILC-17.1 release suppresses p53/CEP-1 and allows reproductive growth; decreased ILC-17.1 signaling activates p53/CEP-1-dependent transcription and metabolic programs, leading to the reversible arrest of larvae as quiescent dauers. Our studies suggest an ancestral function of IL-17 is linking nutrient availability to energy metabolism and growth. They reveal a DNA damage-independent function of p53/CEP-1 in invertebrate development. Finally, our studies support the existence of a previously undescribed dauer pathway in *C. elegans*.

Abstract. During metazoan development, how cell division and metabolic programs are coordinated with nutrient availability remains unclear. Here, we show that nutrient availability signaled by the neuronal cytokine, ILC-17.1 switches *C. elegans* development between reproductive growth and dormancy by controlling the activity of the tumor suppressor p53 ortholog, CEP-1. Specifically, upon food availability, ILC-17.1 signaling by amphid neurons promotes glucose utilization and suppresses CEP-1/p53 to allow growth. In the absence of ILC-17.1, CEP-1/p53 is activated, upregulates cell-cycle inhibitors, decreases phosphofructokinase and cytochrome C expression, and causes larvae to arrest as stress-resistant, quiescent dauers. We propose a model whereby ILC-17.1 signaling links nutrient availability and energy metabolism to cell cycle progression through CEP-1/p53. These studies describe ancestral functions of IL-17s and the p53-family of proteins and are relevant to our understanding of neuroimmune mechanisms in cancer. They also reveal a DNA damage-independent function of CEP-1/p53 in invertebrate development and support the existence of a previously undescribed *C. elegans* dauer pathway.

28 During metazoan development, nutrient availability is coordinated with the division, growth and
29 metabolic activity of individual cells through cell-cell communication. This is also the case in the
30 invertebrate *C. elegans*, a free-living bacterivore, which displays a dramatic developmental
31 plasticity to ensure that its growth and reproduction match available resources(1-10). When *C.*
32 *elegans* larvae hatch under optimal conditions (at 20°C, low population densities, on abundant
33 food) they develop continuously into reproducing adults. However, if they hatch under suboptimal
34 conditions, such as in the paucity of food, at high population densities, or high ambient
35 temperatures, larvae implement an alternative developmental program and arrest as quiescent,
36 stress-resistant larvae called 'dauer' larvae. Dauer larvae display metabolic and organismal
37 phenotypes specialized for dispersal and survival, and can remain arrested in this state for months
38 to resume development into reproductive adults when favorable conditions return(1-10). Previous
39 studies have identified molecular pathways that mediate the dauer decision, showing that growth
40 promoting molecules like insulins, transforming β growth factor (TGFβ/DAF-7) and lipid based
41 dafachronic acid hormones are released by sensory neurons and other cells to license continued
42 development; adverse environments inhibit these growth promoting signals and trigger dauer
43 arrest(1-11). A number of quantitative trait loci (QTL) also modulate dauer (12). Yet, how the
44 dauer entry decision results in a coordinated change in cell fates across different tissues and is
45 linked with the systemic shut-down of anabolic pathways remains poorly understood.
46
47 An important group of proteins that mediate cell-cell communication and metabolism in metazoa
48 are secreted proteins called cytokines(13, 14). The IL-17 cytokines constitute a family of
49 proinflammatory cytokines, highly conserved across animal phyla. In mammals, these cytokines
50 are released by specialized immune cells to activate immune surveillance, enhance barrier
51 function, promote wound healing, and play crucial immunometabolic roles in maintaining energy
52 homeostasis(15). In humans, IL-17s also promote cancers and autoimmune disease such as
53 psoriasis(16, 17). Here, we show that the *C. elegans* IL-17 ortholog, ILC-17.1, signals food

54 availability, and coordinates cell division with metabolism by controlling the activity of the *C.*
55 *elegans* tumor suppressor p53 ortholog, CEP-1. Specifically, neuronal ILC-17.1 suppresses CEP-
56 1/p53 activity in the presence of food to license growth. Upon the loss of ILC-17.1 signaling, CEP-
57 1/p53 is activated, and remarkably, this switches whole organism development from continuous
58 growth to dormancy. The p53-like tumor suppressor genes are found in all multicellular animals
59 where they prevent the transmission of damaged DNA by activating a multifaceted program that
60 controls cell cycle checkpoints, mediates reversible growth arrest or apoptosis, and controls
61 metabolic flux (18-22). Our studies show that these functions of CEP-1/p53 also act, in the
62 absence of DNA damage, to control developmental quiescence of *C. elegans*, suggesting that
63 the developmental function of the p53- gene family could have shaped their evolution(23-25).
64

65 **Results**

66 **ILC-17.1 is released by *C. elegans* amphid neurons in response to food and prevents dauer**
67 **arrest.**

68 *C. elegans* express three IL-17 orthologs(26, 27). Of these, ILC-17.1 is a neuromodulator that is
69 expressed by a subset of specialized sensory neurons with epithelial properties called amphid
70 neurons, that are exposed to the environment(26-28). We discovered that a deletion in *ilc-17.1,*
71 *syb5296,* that removes almost all the coding sequence (2173bp out of 2980 bp; Supplementary
72 Fig. S1a) and abolishes mRNA expression (Supplementary Fig. S1b) caused larvae to
73 constitutively enter the dauer state (Figure 1a, b; Supplementary Fig. S1c, d). Dauer larvae can
74 be identified by their growth arrest and distinct morphology characterized by specialized cuticular
75 structures called alae, a constricted pharynx, arrested germ line, decreased pharyngeal pumping
76 rates, and detergent (1% SDS) resistance(3-9). *ilc-17.1*(*syb5296*)X dauer larvae displayed all
77 these features (Supplementary Fig. S1e-j). Even at 20°C, *ilc-17.1* deleted larvae entered the
78 dauer state transiently: approximately 30% (31.2 ±5%) were SDS-resistant 48 hours post-
79 hatching on OP50 bacteria, and most larvae exited dauer and become reproductive adults by 72

80 hrs. (Supplementary Fig. S1c, d). Under the same conditions, none of the wild-type larvae were
81 detergent resistant, nor did they arrest as dauers. However, as with other mutations that promote
82 dauer entry(3, 4, 29), the dauer arrest of *ilc-17.1* deletion mutants was dramatically accentuated
83 at the slightly higher ambient temperature of 25°C, which still supported the growth of all wild-type
84 larvae into reproductive adults, but caused practically 100% of larvae lacking *ilc-17.1* to enter and
85 persist in the arrested dauer state for days (Fig.1a-d).
86
87 *Ilc-17.1* has not been identified in previous genetic screens for dauer pathway genes(3, 5, 30-32).
88 Therefore, although no off-target effects using CRISPR have been observed in *C. elegans* even
89 after whole genome sequencing (33-35), we conducted additional experiments to confirm the role
90 of *ilc-17.1* in dauer entry, by (i) examining the developmental phenotype of another independently
91 generated CRISPR deletion in *ilc-17.1, syb5297* (loss of 2188 bp of 2980 bp; Supplementary Fig.
92 S1a), (ii) backcrossing *ilc-17.1 (syb5296)* mutants, and (iii) downregulating *ilc-17.1* and its
93 receptor(26, 27) in a wild-type (N2) background using RNA interference (RNAi) and auxin-induced
94 degradation (AID). Like *ilc-17.1* (*syb5296*), *ilc-17.1* (*syb5297*) created using a different guide RNA
95 also displayed a completely penetrant dauer arrest at 25°C (Fig. 1a, b; Material and Methods).
96 Not surprisingly, CRISPR alone did not trigger dauer arrest, and a similarly large CRISPR-induced
97 deletion in a related gene *F25D1.3, syb7367* (loss of 1475 bp of 1642 bp) did not trigger dauer
98 arrest (Supplementary Fig. S1k). *ilc-17.1* (*syb5296*) larvae continued to arrest as dauers after
99 they were backcrossed twice into a wild-type background (Supplementary Fig. S1k). In addition,
100 RNAi-mediated downregulation of *ilc-17.1* in wild-type (N2) animals, but not control RNAi
101 treatment, caused a small but significant number of larvae to arrest as SDS-resistant dauers
102 (Supplementary Fig. S1l). ILC-17.1 signals though cytokine receptors which in *C. elegans*
103 consists of ILCR-1/ILCR-2(26, 27). The ILCR-2 subunit is widely expressed and readily visible in
104 the pharynx, hypodermis, intestine, neurons and germ line, as determined using a bicistronic SL2
105 cassette to tag the *ilcr-2* receptor at its endogenous locus with GFP (Supplementary Fig. S2a-g).

106 Downregulation of *ilcr-2* through RNAi in wild-type larvae also caused over one-third, 39.6% ±
107 4%, to arrest as dauers and did not alter the dauer entry of *ilc-17.1* deleted larvae (Fig. 1e). RNAi
108 is generally insufficient to induce dauer arrest even with known dauer pathway genes(3).
109 Therefore, the RNAi-induced dauer entry of larvae exposed to *ilc-17.1* or *ilcr-2* RNAi was not only
110 statistically significant, but also strongly supportive of the role of the *ilc-17.1* pathway in dauer.
111
112 *ilcr-2* RNAi downregulated *ilcr-2* expression across all somatic and germline tissues, albeit to
113 variable extents (Supplementary Fig.S2h-m). Therefore, as additional confirmation, and to
114 identify the tissues where ILCR-2 signaling was required to promote continuous development, we
115 used the AID system to degrade the endogenous ILCR-2 receptor in individual tissues (Fig. 1f).
116 We targeted the nervous system (using the *rgef-1p* promoter), pharynx (*myo-2p*), hypodermis
117 (*col-10p)*, muscle (*unc-54p*), all somatic cells (*eft-3p*) and the germ line (*mex-5p*) individually,
118 using animals that expressed Transport Inhibitor Response 1 (TIR1) in these tissues and
119 endogenous *ilcr-2* fused to an AID degron. Degradation of ILCR-2 in the pharynx or in the nervous
120 system alone caused some larvae to arrest as dauers (Fig. 1g). Degradation of ILCR-2 in the
121 muscle, hypodermis or germ line alone had no effect (Fig. 1g). Blue Fluorescent Protein (BFP),
122 which served as a proxy for AID, was reduced to undetectable levels upon auxin exposure in a
123 similar percentage of larvae in all cases (Supplementary Fig. S2n), and thus did not explain the
124 differences in dauer entry seen upon ILCR-2 degradation in the different tissues. Control larvae
125 of the same genotype, not exposed to auxin, did not arrest as dauers. Thus, the loss of ILCR-2
126 receptors in the nervous system or pharynx was sufficient to induce the dauer arrest in a subset
127 of animals.
128
129 Surprisingly, degrading ILCR-2 using TIR1 expressed under the pan-somatic *eft-3* promoter,
130 which is expressed in somatic cells such as neurons, pharyngeal cells, intestine, hypodermis, and
131 muscle, but not in the germ line, was less effective in inducing dauer arrest than *ilcr-2* RNAi, or

132 degradation in the pharynx or nervous system alone: only 1.9 ± 0.8 % arrested as dauers
133 compared to 39.6% ± 4% with *ilcr-2* RNAi, and 16.3 ± 1.1 % and 11.3 ± 1.5 % upon neuronal or
134 pharyngeal AID (Fig. 1g). A logical hypothesis which requires future testing is that downregulation
135 of ILCR-2 elicits complex tissue cross-talk, whereby germline-specific ILCR-2 degradation alone,
136 while insufficient to trigger dauer arrest (e.g. *mex-5p::TIR1*), might synergize with knock-down in
137 somatic tissue to promote dauer arrest mirroring the effects observed with *ilcr-2* RNAi. Likewise,
138 decreased ILC-17.1 signaling in some tissues upon pan-somatic ILCR-2 degradation using the
139 *eft-3* promoter, might antagonize the dauer-inducing effects of degradation in the pharynx or
140 nervous system. Although more in-depth studies are required to understand the tissue-
141 requirements, taken together, these observations support the role of ILC-17.1 signaling through
142 the ubiquitously expressed ILCR-2 receptors in the dauer pathway. They also suggest that during
143 normal development ILC-17.1 signaling may elicit complex inter-tissue crosstalk to promote the
144 growth of larvae into reproducing adults or trigger their dauer arrest.
145
146 *ilc-17.1* mRNA expression is restricted to a small subset of neurons: only a pair of amphid sensory
147 neurons (ASE) and two pairs of interneurons (AUA and RMG) expressed transgenic *ilc-17.1*
148 reporter constructs in a previous study (26), and a few dye-filling amphid neurons expressed
149 mCherry as a bicistronic SL2 cassette along with *ilc-17.1* mRNA from the endogenous *ilc-17.1*
150 locus, in our studies (Fig. 1h; Supplementary Fig. S3a-g). The dauer phenotype of *ilc-17.1*
151 deletion mutants could be rescued by re-expressing *ilc-17.1* under the control of its own promoter
152 (Fig.1b and Supplementary Fig. S3h; see Supplementary Fig. S3i for expression levels of rescue
153 construct in comparison to the endogenous gene). The extent of rescue was significant, although
154 modest on OP50 (Fig.1b), but was higher on HT115 bacteria where ILC-17.1 re-expression
155 rescued approximately 63.6% of the *ilc-17.1* deleted larvae from dauer arrest (Supplementary
156 Fig. S3h). Re-expressing *ilc-17.1* ectopically in *ilc-17.1* deleted larvae, remote from its normal
157 site of expression, using the muscle-specific *unc-54* promoter (Supplementary Fig. S3j-t), also

158 rescued dauer arrest of *ilc-17.1* deleted larvae (Fig.1b and Supplementary Fig. S3h), and RNAi
159 mediated downregulation of *ilcr-2* reduced the percentage of *ilc-17.1* larvae that were rescued by
160 ectopically re-expressing ILC-17.1 (Supplementary Fig. S3h). The diet-dependence of rescue
161 was not observed with ectopically expressed *ilc-17.1* (Fig.1b and Supplementary Fig. S3h). The
162 effects of AID-induced knockdown of ILCR-2 in different tissues were also similar when larvae
163 were fed HT115 bacteria instead of OP50 (Supplementary Fig. S3u and Fig.1g). This suggested
164 that the role of ILC-17.1 signaling in dauer might be related to food, a prominent modulator of the
165 dauer decision(3-9), and that the ILC-17.1 ligand, and perhaps not the *ILCR-2* receptor *per se*,
166 could be responsive to the food signals.
167
168 To directly examine whether ILC-17.1 responded to food, we immunolocalized ILC-17.1 protein
169 tagged at its endogenous locus using a HA-tag, in larvae that were hatched in the absence or
170 presence of food (OP50; Fig 1h-l). While the site of *ilc-17.1* expression was not apparently altered
171 by the presence of food, as detected by mCherry expression that remained restricted to amphid
172 neurons (Fig. 1i, k), ILC-17.1 protein was present outside the amphid neurons, concentrated in
173 the pharynx when larvae were exposed to food (Fig 1l), but not when larvae hatched in the
174 absence of food (Fig.1j, quantification in Supplementary Fig. S3v; negative controls Fig. 1m,n).
175 This suggested that ILC-17.1 protein was released from its site of expression in amphid neurons,
176 to be either selectively translated or retained by the pharynx in response to food signals [we could
177 not reliably detect ILC-17.1 protein in distal tissues such as the intestine or coelomocytes]. The
178 secretion of ILC-17.1 protein was also supported by immunolocalization studies on the muscle-
179 expressed ILC-17.1 protein which, although expressed under a well-characterized muscle-
180 specific promoter (i.e. *unc-54*), could be constitutively detected outside muscle cells, throughout
181 the animal (Supplementary Fig. S3m-t). This release of the ectopically expressed ILC-17.1 was
182 not obviously affected by the absence of food (Supplementary Fig.S3q-t). These studies together
183 showed that ILC-17.1 was released from its locus of expression in response to food, consistent

184 with its being secreted, and that the ILC-17.1 signal, transduced through the ILCR-2 receptors in
185 the neurons and/or pharyngeal muscle, acted cell non-autonomously to control the growth of *C.*
186 *elegans*.
187
188 Sequencing total RNA (RNA-seq) extracted from bleach synchronized larvae grown for 32-36
189 hours at 25°C when *ilc-17.1* mutant larvae were *en route* to dauer arrest, and wild-type larvae
190 were late L2s *en route* to developing into reproducing adults, showed that *ilc-17.1* mutant larvae
191 expressed the molecular signatures of dauer larvae(6, 36-38) that were distinct from wild-type
192 larvae and from *ilc-17.1* deletion mutants that re-expressed ILC-17.1 (Supplementary Figure S4a;
193 Datasets S1-S3). This signature consisted of the downregulation of anabolic processes such as
194 DNA replication and ribosome biogenesis (Fig. 1o), upregulation of catabolic processes and
195 stress responses such as autophagy, fatty acid metabolism, glutathione metabolism, and
196 xenobiotic defense pathways (Fig. 1p) and the expression of dauer-specific collagen genes that
197 differ from the collagens expressed during continuous development(39) (Fig. 1q; Dataset S4). We
198 evaluated whether the gene expression profile of the *ilc-17.1* deleted dauers was similar to
199 previously described *C. elegans* dauers that accumulate in the population upon starvation or
200 crowding by comparing our RNA-seq data with published datasets (38). Consistent with a role
201 for ILC-17.1 in signaling nutrient availability, the expression profile of *ilc-17.1* deleted larvae was
202 more closely correlated to dauer larvae generated by starvation(38) (Supplementary Fig. S4b),
203 compared to ascaroside induced dauers(37) (Supplementary Fig. S4c; Datasets S5, S6). These
204 differences were surprising and suggest that the trigger and route of dauer entry could determine
205 their gene expression profiles (40, 41).
206
207 **ILC-17.1 loss activates CEP-1/p53 to trigger dauer entry through the activation of DAF-**
208 **16/FOXO, DAF-3/SMAD-DAF-5/Ski complex and steroid hormone pathways.**

209 To understand how the loss of ILC-17.1 was triggering dauer entry we first considered the
210 possibility that, because of its role as a neuromodulator(26), the lack of *ilc-17.1* prevented larvae
211 from finding or ingesting food. However, this did not seem to be the case (Supplementary Fig. S5;
212 see Extended Text 1 for details). Therefore, to answer how the loss of ILC-17.1 triggered dauer
213 entry, we adopted a genetic approach (2-11, 29). In *C. elegans*, insulins released in the presence
214 of food act through the sole insulin-like receptor, DAF-2, antagonize the activation of the Forkhead
215 transcription factor DAF-16, and promote continuous growth: loss of DAF-2 signaling leads to
216 DAF-16 activation and dauer entry(2-11, 29). Likewise, TGFβ/DAF-7 ligands antagonize the
217 DAF-3/SMAD-DAF-5/Ski transcription factor complex to permit continuous growth: inhibition of
218 DAF-7 activates DAF-3/SMAD-DAF-5/Ski and leads to dauer arrest(2-11, 29). Both insulins and
219 TGF-β promote the synthesis of sterol based dafachronic acid (DA) hormones that act through
220 the nuclear hormone receptor, DAF-12, to support adult development(2-11, 29). Loss of DA
221 pathway components also triggers dauer arrest, and providing exogenous DA to, or decreasing
222 DAF-12 activity in, animals deficient in insulin or TGFβ signaling, can bypass their dauer arrest(3,
223 42). Finally, a mutation in a transmembrane guanylyl cyclase *daf-11* that causes chemosensory
224 defects also triggers dauer arrest(3, 43). *ilc-17.1* deletion mutants lacked obvious chemosensory
225 defects (Supplementary Fig. S5; Extended Text 1) and continued to arrest as dauers on 5mM 8-
226 Bromo-cGMP, which modestly rescues *daf-11*-associated dauer formation(3, 43) (Supplementary
227 Fig. 6a). Therefore, to identify signal transduction pathways through which the loss of ILC-17.1
228 signaling controlled the dauer decision, we examined its genetic interactions with *daf-16, daf-5*,
229 and DA signaling.
230
231 A *daf-16* loss of function mutation*, mu86*(44)*,* completely suppressed dauer formation in animals
232 lacking ILC-17.1, indicating that activation of DAF-16 was one mechanism responsible for their
233 dauer arrest (Fig. 2a). The activation of DAF-16 in animals lacking ILC-17.1 could be quantified
234 by an increase in the proportion of larvae with DAF-16::GFP(45) positive intestinal nuclei even at

235 20°C (Fig. 2b-d), and the upregulation of DAF-16 target genes(46, 47) both at 20°C
236 (Supplementary Fig. S6b) and 25°C (Fig.2e). DAF-16 activation could be suppressed by re-
237 expressing ILC-17.1 in *ilc-17.1* deletion mutants under its endogenous promoter, or ectopically,
238 under the muscle-specific promoter (Fig.2e). Surprisingly, a loss of function mutation in *daf-5*,
239 *e1386*(48) also completely suppressed the dauer arrest of *ilc-17.1* mutant larvae (Fig. 2f), and
240 exposing *ilc-17.1* deficient larvae to 50 nM exogenous Δ7-dafachronic acid (42), partially but
241 significantly suppressed their dauer arrest (Fig 2g). The activation of DAF-16/FOXO and DAF-
242 3/SMAD-DAF-5/Ski by the loss of ILC-17.1 was not simply because *ilc-17.1* deleted larvae were
243 deficient in the expression of insulin signaling and TGFβ/ DAF-7 signaling pathway components,
244 as determined by expression levels of the signaling pathway components and transcriptional
245 reporters [Supplementary Fig S7; Datasets S7, S8, see Extended Text 2 for details]. The dauer
246 arrest of *daf-2* (*e1370*)(49), could not be rescued by ILC-17.1 overexpression, suggesting that
247 ILC-17.1 did not act genetically downstream of *daf-2* (Supplementary Fig. S8a). Thus, it appeared
248 that ILC-17.1 acted upstream of both DAF-16/FOXO and DAF-3/SMAD-DAF-5/Ski (and likely,
249 DAF-9/DAF-12), but not downstream of DAF-2, to modulate dauer entry.
250
251 This was curious, since DAF-16/FOXO and DAF-3/SMAD-DAF-5/Ski are thought to act
252 independently, and in parallel to modulate the *C. elegans* dauer decision(3, 5). Therefore, to
253 identify mechanism(s) that could activate both pathways in *ilc-17.1* deleted larvae, we conducted
254 RNAi knockdown of candidate genes known to interact with these dauer effectors (50-57), and
255 asked which, if any, also rescued the dauer entry of *ilc-17.1* larvae (Supplementary Fig. S8b). We
256 considered only the positive hits, due to the variable penetrance of RNAi. Amongst the positive
257 candidates, we found most interesting, *cep-1*, the *C. elegans* ortholog of p53(58, 59), since p53-
258 family of proteins restrain cell cycle progression and alter metabolism, both cardinal features of
259 dauer entry. Indeed, a deletion in *cep-1*, *gk138*, rescued the dauer arrest of *ilc-17.1* deletion
260 mutants and nearly all (98%) of *cep-1;ilc-17.1* double mutant larvae grew into reproductive adults

261 (Fig 2h-j), suggesting that CEP-1/p53 was also responsible for the dauer phenotype of *ilc-17.1*
262 mutants, and was activated.
263
264 In mammalian cells, p53 activation occurs through an increase in p53 protein levels due to its
265 escape from constitutive degradation by the E3 ubiquitin ligase MDM2(18, 20, 60). Although the
266 *C. elegans* genome lacks MDM2 orthologs, CEP-1/p53 activation through translational and
267 posttranslational modifications has been reported (61, 62). We therefore used Western analysis
268 of FLAG-tagged endogenous *C.* elegans CEP-1/p53 to test whether CEP-1/p53 was activated in
269 *ilc-17.1* mutant larvae, as implied by the rescue. This was the case: in *ilc-17.1* deleted larvae,
270 CEP-1::FLAG levels increased by 2-fold, levels similar to that seen upon gamma irradiation, which
271 also activates CEP-1/p53, and was used as a positive control (Fig 3a) (63, 64). Accordingly,
272 overexpressing CEP-1 alone, even to a modest 1.5-fold level over wild type (see Supplementary
273 Fig. S9a for *cep-1 o/e* mRNA levels), was sufficient to arrest growth and promote an almost
274 completely penetrant dauer phenotype (Fig. 3b-d). CEP-1 overexpression was achieved by
275 crossing out the *cep-1 lg12501* deletion mutation from a widely used transgenic strain expressing
276 functional, fluorescently tagged, CEP-1, CEP-1::GFP, under its own promoter (61, 65, 66). In the
277 *cep-1*(*lg12501*) strain, CEP-1::GFP is the only source of CEP-1/p53, rescues *cep-1* (*lg12501*)
278 apoptosis defects and is expressed at half the levels of wild type (Supplementary Fig. S9a; *cep-*
279 *1* mRNA levels). CEP-1::GFP did not induce dauer arrest in the *cep-1, lg12501* deletion
280 background (Fig. 3b), indicating that *cep-1* expression levels, and not the GFP tag, was
281 responsible for the dauer arrest of CEP-1::GFP overexpressing larvae . The overexpression of
282 CEP-1/p53 phenocopied the *ilc-17.1* deletion, not only causing all larvae to arrest as dauers at
283 25°C, but also prompting transient dauer entry at 20°C, as assessed by SDS-resistance
284 (Supplementary Fig. S9b). RNA-seq analysis showed that genes differentially expressed in CEP-
285 1/p53 overexpressing larvae *en route* to their dauer arrest, significantly overlapped with those
286 expressed in larvae lacking ILC-17.1 (Fig. 3e, padj.< 0.05; Datasets S9, S10). CEP-1/p53

287 overexpressing larvae also upregulated dauer-specific collagens (Supplementary Fig. S9c;
288 Dataset S4), downregulated anabolic pathways (Supplementary Fig. S9d), and upregulated
289 catabolic pathways (Supplementary Fig. S9e). In addition, between 15 hours to 32 hours post-
290 hatching at 25°C, CEP-1/p53 overexpressing larvae and *ilc-17.1* deletion mutants showed a
291 remarkably constant gene expression profile, and only 340 and 34 genes respectively changed
292 expression ($p<0.05$), compared to the > 10,000 genes that were either upregulated or
293 downregulated in wild-type larvae and *cep-1;ilc-17.1* double mutant larvae that *en route* to
294 becoming reproductive adults (PCA analysis; Supplementary Fig. S9f; Dataset S11). The
295 upregulation of known CEP-1/p53 targets (63, 64, 67, 68), the BH3-only proteins *egl-1* and *ced-*
296 *13*, in the *ilc-17.1* deletion mutants, in a *cep-1*-dependent manner, at both 20°C and 25°C, further
297 confirmed CEP-1/p53 activation in the absence of ILC-17.1 (Fig 3f and Supplementary Fig. S10a).
298 The upregulation of CEP-1/p53-targets in *ilc-17.1* deletion mutants could be suppressed by re-
299 expressing ILC-17.1 under its endogenous-, or muscle-specific promoters (Fig 3f; Supplementary
300 Fig. S10a). In addition, Chromatin Immunoprecipitation followed by quantitative PCR (ChIP-
301 qPCR) using FLAG tagged *cep-1* animals showed that the loss of *ilc-17.1* increased CEP-1/p53
302 binding at promoter regions of *egl-1* and *ced-13*, and the increased occupancy was abrogated
303 upon re-expressing ILC-17.1 (Fig. 3g, h).
304
305 Like in the ILC-17.1 deficient animals, the dauer arrest of larvae overexpressing CEP-1 was
306 dependent on DAF-16, DAF-5 and the steroid hormone pathway: downregulating *daf-16*
307 expression by RNAi (Fig. 4a), crossing CEP-1/p53 overexpressing larvae into *daf-5*, *e1386*, or
308 treatment with 50nM exogenous Δ7-dafachronic acid, all suppressed their dauer arrest (Fig. 4b).
309 In accordance, DAF-16 target genes were also upregulated in larvae overexpressing CEP-1/p53
310 at both 25°C (Fig 4c) and 20°C (Supplementary Fig. S10b). Differentially expressed genes in
311 CEP-1/53 overexpressing larvae overlapped with published gene expression profiles of *daf-2*
312 *(e1370)* and active DAF-16 (Supplementary Fig. S10 c,d; Datasets S12, S13). In addition, and

313 most convincing, the upregulation of *daf-16* target genes in *ilc-71.1* deletion mutant larvae was
314 *cep-1* dependent at both 25°C and 20°C (Fig 4c; Supplementary Fig. S10b). CEP-1/p53
315 activation-induced dauer entry appeared to be somewhat specific to reduced ILC-17.1 signaling,
316 as the dauer arrest of *daf-2*(*e1370*) larvae that occurred due to reduced insulin signaling did not
317 depend on *cep-1* (Supplementary Fig. S10e). Moreover, in agreement with previous reports(69,
318 70), *cep-1* was not required for dauer induction at high temperatures as *cep-1* (*gk138*) larvae
319 could enter dauer at 27°C just like wild-type animals (Supplementary Fig. S10f). Taken together,
320 these results showed that ILC-17.1 normally acted to represses CEP-1/p53 transcriptional activity.
321 Upon loss of ILC-17.1 signaling, CEP-1/p53 was activated, in turn activated DAF-16/FOXO (and
322 perhaps DAF-3/SMAD-DAF-5/Ski and DAF-12) to trigger the dauer arrest of *ilc-17.1* deletion
323 mutants. However, the ILC-17.1/CEP-1 dauer axis appeared independent of the insulin-like
324 receptor, *daf-2*, *per se*.
325
326 **CEP-1/p53 directly or indirectly controls cell cycle progression.**
327 A conserved function of the p53-family of proteins is to restrain cell cycle progression. In *C.*
328 *elegans*, most cell divisions are completed during embryogenesis, but a subset of somatic and
329 germ line cells divide and differentiate post-embryonically, and these cells arrest during dauer
330 entry(71-76) (77, 78). (79-86). We therefore tested whether CEP-1/p53 activation upon loss of
331 ILC-17.1 was participating in the arrest of cell cycle progression during postembryonic
332 development. Indeed, *ilc-17.1* deleted larvae upregulated mRNA levels of cell cycle inhibitors *cki-*
333 *1,* one of the two p21 homologs, and *phg-1,* the *C. elegans* homologue of Growth arrest-specific
334 1 (Gas1) (Fig 4d). These are known to regulated by CEP-1/p53 (87). *phg-1,* but not *cki-1,* was a
335 direct target of CEP-1/p53, in *ilc-17.1* deletion mutants, which displayed increased CEP-1/p53
336 occupancy at the *phg-1* promoter (Fig. 4e; Supplementary Fig. S11a). Again, as with the other
337 CEP-1/p53 targets, the increased expression of *cki-1* and *phg-1,* and the increased occupancy at
338 the *phg-1* promoter was restored to wild-type levels upon re-expressing ILC-17.1 (Fig. 4d, e).

339 Surprisingly, downregulation of *phg-1* and *cki-1* by RNAi modestly, but significantly, rescued
340 dauer arrest in *ilc-17.1* deletion mutants and CEP-1/p53 overexpressing larvae and allowed a
341 small number of larvae to develop into adults (Supplementary Fig. S11b). Crossing *ilc-17.1*
342 deletion mutants into *phg-1* deletion mutants, *ok2741* also resulted in a rescue and ~40% escaped
343 dauer arrest and grew into reproductive adults (Fig. 4f, g). In addition, a proportion of *ilc-17.1*
344 deletion mutant and CEP-1/p53 overexpressing larvae that appeared morphologically dauer,
345 displayed modest but significant non-dauer physiological traits on *phg-1* and *cki-1* RNAi such as
346 increased rates of sporadic pumping (Supplementary Fig. S11c; wild-type L2 were used as
347 controls), suggesting there may also occur a wider, albeit incomplete, dauer rescue in some
348 tissues. The dauer arrest of *daf-2* mutant larvae which did not depend on *cep-1,* was also not
349 rescued upon downregulating *phg-1* or *cki-1*, nor were the pumping rates of *daf-2* dauers altered
350 (Supplementary Fig. S11 b,c). Although we cannot distinguish at this time, whether the
351 downregulation of the cell cycle inhibitors allowed larvae to exit dauer, or suppressed dauer entry
352 and complete arrest, these data showed that loss of ILC-17.1 signaling or overexpressing CEP-
353 1/p53 upregulated CEP-1/p53-dependent cell cycle inhibitors, and this increase appeared to be
354 one mechanism responsible, at least in part, for the dauer arrest.
355
356 **ILC-17.1 links glucose metabolism to CEP-1/p53 activity.**
357 Mammalian p53 plays a central roles in energy metabolism and, in turn, can be activated by
358 energy deprivation or limited glucose, through signaling by AMP-activated protein kinase (AMPK)
359 or Mammalian target of rapamycin (mTOR) pathways (88, 89). Therefore, the responsiveness of
360 ILC-17.1 to food signals suggested the intriguing possibility that the loss of ILC-17.1 signaling
361 activated CEP-1/p53 because of energy deprivation, and this could link nutrient availability to
362 metabolism and cell cycle progression. AMPK did not appear to be activated in *ilc-17.1* deleted
363 animals (Supplementary Fig. S12a), nor was mTOR activity obviously reduced (Supplementary
364 Fig. S12b). However, ILC-17.1 signaling did appear to link glucose utilization to developmental

365 progression, since downregulating *fgt-1,* the main Glucose transporter (GLUT) responsible for
366 glucose absorption in *C. elegans*(90), decreased the extent of dauer-rescue conferred by re-
367 expressing ILC-17.1 in *ilc-17.1* mutant larvae (Fig. 5a), and increased the numbers of *ilc-17.1*
368 deletion mutant larvae that arrested as dauers at 20°C (Fig. 5b). Conversely, extra glucose(91)
369 suppressed the dauer arrest of approximately 30% *ilc-17.1* deficient larvae (Fig. 5c;
370 Supplementary Fig. S12c), suggesting that the normal amounts of glucose available in the diets
371 of *C. elegans* larvae was insufficient for *ilc-17.1* larvae to develop into adults. Consistently,
372 decreasing glucose import through *fgt-1* RNAi once again, lowered the percentage of larvae that
373 were rescued by the extra glucose (Supplementary Fig. S12d), and no rescue was observed on
374 the non-hydrolysable glucose analog 2-Deoxy-d-glucose (2-DOG; Supplementary Fig. S12e)
375 which cannot undergo glycolysis and does not enter the metabolic pathway. The same
376 concentrations of glucose could not rescue *daf*-2 larvae that arrested as dauers (Fig 5c). We ruled
377 out non-specific effects of glucose rescue by testing the role of increased ROS or other
378 supplements (Supplementary Fig S12e-f; see Supporting Information; Extended Text 3 for
379 details). Downregulating *fgt-1* in wild-type larvae, while not sufficient to trigger dauer arrest,
380 modestly increased the expression of CEP-1/p53 target *egl-1* (but not *ced-13*; Supplementary
381 Fig. S12g). Thus, these data supported the possibility that the activation of CEP-1/p53 upon the
382 loss of ILC-17.1 could, at least in part, occur due an impairment in the *ilc-17.1* deleted larvae's
383 ability to utilize glucose.
384
385 Glucose supplementation also rescued dauer arrest of CEP-1/p53 overexpressing larvae (Fig 5c;
386 Supplementary Fig. S10c), arguing that decreased glucose intake in the absence of ILC-17.1 was
387 not a consequence of CEP-1/p53 activation, but instead acted logically upstream of CEP-1/p53.
388 In agreement, extra glucose suppressed the increased expression of *phg-1* the direct target of
389 CEP-1/p53, and decreased DAF-16/FOXO activation (Fig.5d). Surprisingly, not only did CEP-
390 1/p53 appear to be activated by the inability of *ilc-17.1* to utilize glucose normally, but CEP-1/p53

391 activity, in turn decreased the expression levels of key enzymes involved in glucose
392 metabolism(92): phosphofructokinase-1.2 (*pfk-1.2*), the rate limiting enzyme in glycolysis, and
393 cytochrome *c* (*cyc-2.2*), the complex IV subunit of the mitochondrial electron transport chain
394 responsible. This was visible in the RNA-seq data (Supplementary Figure S13 a-f; Dataset S14)
395 and confirmed by qRT-PCR (Supplementary Figure S13g, Fig. 5e). Moreover, although the
396 downregulation of *pfk-1.2* or *cyc-2.2* alone was not sufficient to induce dauer in wild-type animals,
397 RNAi knockdown of *cyc-2.2* in *ilc-17.1* deleted larvae increased the percentage of dauers under
398 optimal conditions of 20°C, suggesting that CEP-1/p53-dependent decrease of *cyc-2.2* could
399 feedback onto *ilc-17.1* loss to increase dauer propensity (Supplementary Figure S13h). These
400 data, together, suggested that the loss of ILC-17.1 impaired glucose utilization and this activated
401 CEP-1/p53, which, then further limited glucose utilization by downregulating genes important for
402 glycolysis and OXPHOS. Thus, ILC-17 secretion from amphid neurons that occurred in response
403 to food availability appeared to link cell fate decisions with energy metabolism through CEP-1/p53.
404

405 **ILC-17.1 suppresses CEP-1/p53 in *C. elegans* and human epithelial cells.**

406 Our data pointed towards a model whereby ILC-17.1 signaling suppressed CEP-1/p53. Therefore,
407 we tested this directly. Indeed, overexpressing ILC-17.1 in animals also overexpressing CEP-
408 1/p53 inhibited their dauer arrest (Fig. 6a). In addition, since the most-accepted and canonical
409 function of *C.elegans* CEP-1/p53 is in triggering apoptosis in the adult germ line in response to
410 DNA-damage, we also examined whether ILC-17.1 repressed CEP-1/p53's function in apoptosis.
411 As has been previously shown(67), the loss of CEP-1/p53 in *cep-1 (gk138)* adults has negligible
412 effects on physiological apoptosis, but suppresses the increased apoptosis that occurs in
413 response to gamma irradiation (Fig. 6b). CEP-1/p53 overexpression, surprisingly, caused a
414 significant increase in physiological apoptosis, and a marked increase in irradiation-induced
415 apoptosis, both of which could be suppressed by also overexpressing ILC-17.1 (Fig 6b).
416 Overexpressing *ilc-17.1* in a wild-type background also decreased physiological and irradiation-

417 induced apoptosis, but this effect was variable and did not reach significance (average nos. of
418 apoptotic cells in non-irradiated N2 v ILC-17.1 overexpressing animals were 3.56 ± 1.3 and 2.53
419 ± 1.1 cells, and upon irradiation, increased to 7.1 ± 1.8 in N2, and 5.72 ± 2.2 in IL-17
420 overexpressing animals). For reasons that remain to be understood, ilc-*17.1* deletion did not alter
421 apoptosis in the adult germ line, perhaps reflecting a different function post-development. IL-17
422 could also modestly repress p53, autonomously, in mammalian cells (Supplementary Fig S14a-
423 b; see Extended Text 4 for details). Together, these data suggest that the inhibition of CEP-
424 1/p53's activity could be a conserved function of IL-17s.
425

426 **Discussion**

427 Here we show roles for the interleukin 17 (IL-17) family of cytokines and p53 in the development
428 of an invertebrate species, *C. elegans*. Our data support a model whereby ILC-17.1 signaling of
429 food availability by amphid neurons ensures the continuous growth of larvae into reproductive
430 adults under favorable conditions through suppression of CEP-1/p53. IL-17s play broad-ranging
431 immunometabolic roles in mammals and are one of the most conserved proinflammatory
432 cytokines among animal phyla. Thus, their ancestral role in signaling nutrient availability as in *C.*
433 *elegans* may be broadly conserved. Our data also reveal that reduced ILC-17.1 signaling,
434 expected to occur when food is scarce, activates CEP-1/p53, to trigger dauer arrest through the
435 well characterized dauer activating pathways, DAF-16/FOXO, DAF-3/SMAD-DAF-5/Ski and also,
436 perhaps steroid hormone signaling. In its role in promoting dauer arrest in *C. elegans*, CEP-1/p53
437 inhibits cell cycle progression, and modulates metabolic flux by directly or indirectly controlling the
438 levels of phosphofructokinase (*pfk*-1) and cytochrome C (*cyc-2.2*). Notably, these are also
439 mechanisms by which p53 restrains tumorigenesis. In mammals too, uncontrolled p53 activity is
440 associated with a developmental syndrome through its effects on cell cycle progression, apoptosis
441 and the migration of neural crest cells(25). We therefore cautiously propose that the ancestral

442 roles of the p53 gene-family in modulating development could have the driving force in their
443 evolution.

444

445 While, there remain several puzzling aspects associated with this study, our data indicate that
446 there may exist a previously undiscovered *C. elegans* dauer pathway. The dauers formed by *ilc-*
447 *17.*1 deletion, or the modest 1.5X increase in CEP-1/p53 expression, display all the cardinal
448 morphological and physiological features of dauers, including SDS-resistance, decreased
449 pumping rates, presence of alae, changes in collagens, upregulation of catabolic and
450 downregulation of anabolic genes, and the ability to remain arrested for days to weeks as dauers.
451 Nevertheless, they also differ in some respects from the well-studied dauers formed through
452 decreased insulin signaling (*daf-2*), and other pathways, in that, unlike previously studied dauers,
453 a modest, but significant percentage of *ilc-17.1* dauers larvae bypass or are rescued from dauer
454 upon downregulating cell cycle inhibitors such as *phg-1*, or when fed extra glucose. This suggests
455 that there may exist different 'types' of dauer larvae. The discovery of new *C. elegans* dauer
456 pathway genes is surprising given the extensive genetic screens that have been conducted(3, 5,
457 30-32). However, genes that require a complete deletion to confer a dauer phenotype, or genes
458 that control development through complex and antagonistic tissue specific effects, as possible for
459 *ilcr-2*, could have been missed. In this regard, two other deletions of the *ilc-17.1* exist in the
460 community (*tm5218 and tm5124*). These do not arrest as dauers, but are also not null alleles and
461 express exons 1 and 2 of *ilc-17.1* transcript (Supplementary Figure S14c). However, the *tm5218*
462 deletion removes the predicted beta strands required for the canonical cysteine knot fold of IL-
463 17s and might have arguably been expected to be result in the loss of ILC-17.1 signaling
464 capability, mimic *ilc-17.1* deletion mutants, and arrest as dauers. Although this is not the case,
465 and all *tm5218* homozygotes escape dauer arrest, a variable, but significant percentage of trans-
466 heterozygotes for *ilc-17.1(tm5218)* and *ilc-17.1*(*syb5296*) larvae arrest as dauers, as confirmed

467 by PCR genotyping, indicating non-complementation (Supplementary Figure S14d; results from
468 one experiment; dauer arrest varied between 0-75% of F1 trans-heterozygotes; n>10
469 experiments). This observation adds confidence to the role of *ilc-17.1* in dauer, but also reinforces
470 our lack of understanding of the nature and stoichiometry of the IL-17 homo/heterodimers and IL-
471 17-ILCR-2 signaling assemblies in *C. elegans*.
472
473 We hypothesize that ILC-17.1 is secreted upon sensory neuronal activity to control CEP-1/p53
474 activity, but this remains to be shown, and the neuronal circuits identified(93). Nutrient scarcity
475 has shaped much of evolution, and the ability of cells and organisms to sense nutrient availability
476 and prepare in anticipation to pause cell cycle progression and growth and maintain a quiescent
477 state until resources are optimal, has unquestionable selective advantages. For *C. elegans*, like
478 for most organisms, the availability of food is not guaranteed. Neuronal ILC-17.1 signaling
479 appears to be one mechanism which allows the animal to match the cell fate programs and
480 metabolic requirements of the developing larvae with resource availability. Neurons also control
481 dauer entry though TGFβ and insulin signaling. In addition, other stress-responsive
482 transcriptional programs that can be activated autonomously by cells, are also controlled through
483 neuronal signaling in *C. elegans*, allowing the nervous system to coordinate tissue-specific
484 transcriptional and epigenetic responses with organismal physiology and behavior(94-97). The
485 extent to which IL-17s function similarly in mammals remains to be understood (98, 99).

Materials and Methods: Descriptions of strains and methods are included in Supporting Information (SI), Extended Methods. Strains will be available upon request, after publication. The data discussed in this publication have been deposited in NCBI's Gene Expression Omnibus (Edgar et al., 2002) and are accessible through GEO Series accession number GSE218596, , https://www.ncbi.nlm.nih.gov/geo/query/acc.cgi?acc=GSE218596 and GSE229132, https://www.ncbi.nlm.nih.gov/geo/query/acc.cgi?acc=GSE229132

493 **Figure 1: ILC-17.1 signaling of food availability by larval amphid neurons modulates dauer**
494 **arrest.**
495 **(a),** Schematic of experiment. For each experiment, independent samples of 10 day-one adults
496 of each strain laid eggs for two-four hours at 20°C on OP50 lawns. Adults were removed,
497 embryos transferred to 25°C., larval phenotype scored after approximately 48 hr., and
498 categorized as dauers or stage 4 larvae (L4) and/or young adults. SDS-resistance was used to
499 confirm dauers. Extent of crowding on plates was comparable (Representative average
500 numbers of embryos/plates are 64, 68, 56, 46 and 65 for wild type (N2), *ilc-17.1*(*syb5296*) X, *ilc-*
501 *17.1*(*syb5297*) X, *ilc-17.1*(*syb5296*) rescued with *ilc-17.1p::ilc-17.1*, and *ilc-17.1*(*syb5296*)
502 rescued with *unc-54p::ilc-17.1* respectively). *ilc-17.1 rescued (ilc-17.1p)* are *ilc-17.1* deletion
503 mutants expressing extrachromosomal *ilc-17.1* cDNA driven by *ilc-17.1* promoter. *ilc-17.1*
504 rescued *(unc-54p)* are *ilc-17.1* deletion mutants expressing extrachromosomal *ilc-17.1* cDNA
505 driven by *unc-54* promoter. Pearson's Chi-squared test with Yates' continuity correction was
506 used to compare samples in manuscript, unless otherwise stated. Chi-squared, df and p values
507 for the whole experiment and p values for pair-wise comparisons are reported. ***$p < 0.001$,
508 **$p < 0.01$, *$p < 0.05$ and ns, not significant. **(b),** Percentage larvae that arrest as dauers, (*n*=3-
509 12 experiments; Chi-squared = 2359.6, df = 4, p-value < 2.2e-16.). (**c**, **d)**. Representative
510 micrographs 48 hours post-hatching at 25°C: **(c),** wild type (N2) are L4s, **(d),** *ilc-17.1*(*syb5296*)
511 are dauer. Scale bar, 1 mm. **(e)**. Percentage dauers amongst wild type (N2), and *ilc-17.1*
512 mutants on control (L4440) and *ilcr-2* RNAi, (n=3-10 experiments. Chi-squared = 1815.1, df = 7,
513 p-value < 2.2e-16.). **(f),** Schematic of AID experiment to degrade ILCR-2. **(g),** Percentage
514 dauers following tissue specific degradation of ILCR-2. X-axis: tissue specific TIR1 expression,
515 (n=4-6 experiments; Chi-squared = 335.56, df =9 , p-value <2.2e-16). (**h).** Schematic of
516 experiment to localize *ilc-17.1* mRNA and ILC-17.1 protein in the presence and absence of food
517 (OP50). Embryos hatched at 20°C and imaged after 24-36 hours (L1 stage larvae): **(i, k),**
518 Representative micrographs of z-section of pharyngeal region of larvae showing mCherry as

519 proxy for *ilc-17.1* mRNA expression in amphid neurons**. (j, l),** z-section projection showing
520 immunolocalization of ILC-17.1::HA protein. **(i, j)** larvae in absence of food, and **(k, l),** presence
521 of food. **(m, n),** Controls (N2) that do not express HA or mCherry to indicate specificity of the
522 fluorescence signal. (n>3 experiments, 4-5 larvae each). Scale bar, 5μm. (**o),** KEGG
523 enrichments associated with differentially downregulated genes, and (**p**), differentially
524 upregulated genes in *ilc-17.1* mutant larvae. p.adjust <0.05. RNA-seq on 32-36 hr. larvae. (**q),**
525 Heatmap depicting expression levels (log_2 normalized counts) of the major dauer-specific
526 collagens in L2 wild-type (N2) larvae *en route* to adult development, *ilc-17.1* deletion mutants *en*
527 *route* to dauer entry and *ilc-17.1* deletion mutants rescued from dauer with *unc-54p::ilc-17.1.*
528 Bars show mean ± S.E.M. Individual data points in the bar graphs in **b** and **e, g** represent the %
529 dauers/experiment, and the bar graph depicts mean of these percentages. ***$p < 0.001$,
530 **$p < 0.01$, *$p < 0.05$ and ns, not significant
531

532 **Figure 2: Reduced ILC-17.1 signaling acts through DAF-16/FOXO, DAF-3/SMAD-DAF-**
533 **5/Ski complex, steroid hormone signaling and CEP-1/p53 to control dauer arrest.**
534 **(a),** Percent dauers. X-axis: genotype. (*n*=4-8 experiments, Chi-squared = 497.65, df = 1, p-
535 value < 2.2e-16). **(b),** Percent 36 hrs larvae, grown at 20°C showing nuclear DAF-16::GFP**.** *n*=3
536 experiments with 10-15 larvae each. Each data point represents average no. of larvae with
537 nuclear DAF-16::GFP/experiment, (unpaired t-test). Note: experiments were conducted at 20°C,
538 since DAF-16::GFP localized constitutively in intestinal nuclei even in wild-type larvae at 25°C.
539 **(c, d),** representative micrographs of DAF-16::GFP (boxed) in wild type and *ilc-17.1* deletion
540 mutant larvae. Scale bar, 5μm. **(e),** Average *sod-3, mtl-1, and lys-7* mRNA levels in larvae 32-36
541 hr. post-hatching at 25°C. mRNA levels are relative to *pmp-3* and normalized to wild type (N2)
542 values. *n*=4-10 experiments, (unpaired t-test). (**f),** Percent dauers. X-axis: genotype. (*n*=3-5
543 experiments, Chi-squared = 787.3, df = 3, p-value < 2.2e-16). (**g),** Percent dauers in *ilc-17.1*
544 mutants on control (H_2O) and exogenous 50nM Δ7-dafachronic acid (DA), (*n*=3-5 experiments,
545 Chi-squared = 784.32, df = 3, p-value < 2.2e-16). (**h),** Percent dauers, X-axis: genotype (*n*=3-5
546 experiments, Chi-squared = 1029.2, df = 3, p-value < 2.2e-16). **(i, j),** Representative
547 micrographs of **i,** *ilc-17.1* deleted larvae arrested as dauers, and j**,** *ilc-17.1;cep-1* that grew to
548 L4s, 48 hr. post-hatching at 25°C. Scale bar, 1 mm. Bars show the mean ± S.E.M. Individual
549 data points in bar graphs in **a, f-h,** represent the average % dauers/experiment. ***p < 0.001,
550 **p < 0.01, *p < 0.05 and ns, not significant
551

552 **Figure 3: CEP-1/p53 is activated by reduced ILC-17.1 signaling.**

553 **(a), Top**: Representative Western blot showing CEP-1::FLAG and tubulin. Bands on western
554 correspond to numbers in data bars. *cep-1* RNAi used for specificity. Samples constitute 32-36
555 hr. larvae grown at 25°C, except for positive control, irradiated sample (#4; adults). **Bottom**:
556 Average CEP-1 levels quantified relative to tubulin and normalized to control (Ctrl; CEP-
557 1::FLAG in wild-type background). n=4 experiments. (unpaired t-test). (**b),** Percent dauers. X-
558 axis: genotype. (n=3-4 experiments, Chi-squared = 569.35, df = 2, p-value < 2.2e-16). mRNA
559 expression levels in *cep-1* OE and *cep-1 (lg12501)*; CEP-1::GFP were ~1.5X and ~0.5X wild-
560 type levels, respectively, see **Supplementary Fig. S9a**. **(c, d),** Representative micrographs 48
561 hrs. post-hatching at 25°C, of **c,** CEP-1/p53 overexpressing larvae arrested as dauers and **d,**
562 *cep-1 (lg12501)*; CEP-1::GFP L4s. Scale bar, 1 mm. **(e),** Venn diagram depicting overlap
563 between differentially expressed genes (p<0.05) in *ilc-17.1* deletion mutants and CEP-1/p53
564 overexpressing larvae, 32-36 hr. post-hatching at 25°C. p<0.0; hypergeometric test. **(f)**, Average
565 *egl-1* and *ced-13* mRNA levels in 32-36 hr. larvae grown at 25°C. n=6-7 experiments. mRNA
566 levels relative to *pmp-3* and normalized to wild-type (N2) values. (unpaired t-test). **(g, h),** CEP-1
567 occupancy (percent input; CEP-1::FLAG was immunoprecipitated with anti-FLAG antibody) at
568 the promoter proximal regions of **g,** *egl-1* and **h,** *ced-13* in 32-36 hr. larvae grown at 25°C, (**Top,**
569 schematic). X-axis: genotype. n=4 experiments. (unpaired t-test). (**a, g, h**), endogenous *cep-1*
570 was FLAG tagged at its C-terminus using CRISPR/Cas9, crossed into backgrounds noted and
571 probed with anti-FLAG antibody. Bars show the mean ± S.E.M. Individual points in bar graphs in
572 **b** represent the % dauers/experiment. ***p < 0.001, **p < 0.01, *p < 0.05 and ns, not significant.

573

574

575 **Figure 4. CEP-1/p53 acts through DAF-16/FOXO, DAF-3/SMAD-DAF-5/Ski complex and**
576 **cell cycle inhibitors to control dauer entry.**
577 **(a)**, Percent dauers. X-axis: genotype and RNAi treatment: Ctrl, L4440 or *daf-16*. (n=3-4
578 experiments, Chi-squared = 494.22, df = 3, p-value < 2.2e-16). **(b),** Percent dauers. X-axis:
579 genotype and treatment: water (control) and 50nM Δ7-dafachronic acid (DA). (n=3-4
580 experiments, Chi-squared = 982.66, df = 5, p-value < 2.2e-16). **(c),** Average *sod-3, mtl-1, and*
581 *lys-7* mRNA levels in larvae 32-36 hr. post-hatching at 25°C. n=4-10 experiments. (unpaired t-
582 test). **(d)**, Average *cki-1* and *phg-1* mRNA levels in 32-36 hr. larvae grown at 25°C. (**c, d**) mRNA
583 levels were determined relative to *pmp-3* and normalized to wild-type (N2) values. n=4-6
584 experiments. *p < 0.05. (unpaired t-test). **(e),** CEP-1 occupancy (percent input) in 32-36 hr.
585 larvae grown at 25°C, at the promoter proximal region of *phg-1* (**Top,** schematic). X-axis:
586 genotype. n=4 experiments. (unpaired t-test). **(f),** Percent dauers. X-axis: genotype. (n=6
587 experiments, Chi-squared = 826.95, df = 3, p-value< 2.2e-16). **(g),** Representative micrograph
588 48 hrs. post-hatching at 25°C of *ilc-17.1;phg-1* double mutants, showing dauers (arrows) and
589 L4s. Scale bar, 1 mm**. (a**, **b**, **f),** Bar graphs: bars show the mean ± S.E.M, and individual points
590 represent the % dauers/experiment. ***p < 0.001, **p < 0.01, *p < 0.05 and ns, not significant.
591 .
592
593
594
595

596 **Figure 5. Impaired glucose utilization in ILC-17.1 deficient larvae activates CEP-1/p53**
597 **and alters the expression of OXPHOS genes.**
598 **(a), Top**: Schematic of experimental design. **Right**: Percent dauers. X-axis: genotype. Larve
599 treated with control (L4440) and *fgt-1* RNAi. (n= 5 experiments, Chi-squared = 1817.1, df = 5, p-
600 value < 2.2e-16). **(b), Bottom**: Schematic of experimental design. **Right**: Percent SDS (1%)-
601 resistant dauers at 48 and 72 hrs. post-hatching and grown at optimal conditions of 20°C. X-
602 axis: genotype. Larve treated with control (L4440) and *fgt-1* RNAi. (n= 3 experiments, Chi-
603 squared = 206.82, df = 7, p-value < 2.2e-16). **(c), Top**: Schematic of experimental design.
604 **Bottom**: Percent dauers. X-axis: genotype and treatment: Control (H_2O) and 50mM glucose.
605 (n= 3-6 experiments, Chi-squared = 2882.3, df = 5, p-value < 2.2e-16). **(d),** Average *phg-1, sod-*
606 *3 and mtl-1* mRNA levels in 32-36 hr. larvae that arrest as dauers (on H_2O, control) and larvae
607 that bypass dauer (50mM glucose) at 25°C. mRNA levels are relative to *pmp-3* and normalized
608 to wild-type (N2) values. n=3 experiments. (unpaired t-test). **(e),** Average *cyc-2.2* mRNA levels
609 in 32-36 hr. larvae. mRNA levels are relative to *pmp-3* and normalized to the wild-type (N2)
610 values. n=4-6 experiments.. (unpaired t-test). Bars show the mean ± S.E.M. Individual points in
611 the bar graphs in **a, b, c** represent the % dauers/experiment, ***p < 0.001, **p < 0.01, *p < 0.05,
612 ns, non-significant.
613

614 **Figure 6: ILC-17.1 suppresses CEP-1/p53.**

615 **(a),** Percent dauers. X-axis: genotype. (n=4 experiments, Chi-squared = 1245.4, df = 2, p-value
616 < 2.2e-16). **(b), Top:** Schematic of germline-specific apoptosis (apoptotic cells in red) scored
617 with Acridine Orange. **Bottom:** Average numbers of apoptotic cells in day-two adult animals
618 under control, non-irradiated conditions, and upon irradiation with 75 Gy (day-one adults were
619 irradiated). n= 3 experiments, and 12 gonad arms/experiment. (analysis of variance (ANOVA)
620 with Tukey's correction, df=13). Note: p values between N2 vs *ilc-17.1* OE (*unc-54p*), non-
621 irradiated and irradiated are p=0.0192 and p=0.0623, if compared by themselves (unpaired t-
622 test), but do not rise to significance when corrected for the multiple comparisons. Data in all
623 graphs show mean ± S.E.M ***p < 0.001, **p < 0.01.

624

625 A**cknowledgements**

626 We thank the V.P. laboratory, Drs. Sarit Smolikove, Josep Comeron, Anna Malkova and Michael
627 Petrascheck for comments, Dr. Peter Ratcliffe, Oxford, for his generous gift of *CeHIF-1* antibody,
628 and Dr. Mario de Bono, Institute of Science and Technology Austria (ISTA) for *C. elegans* strains.
629 Nematode strains were provided by the Caenorhabditis Genetics Center (CGC) (funded by the
630 NIH Infrastructure Programs P40 OD010440). This work was supported by NIH R01 AG060616
631 (V.P.).

632

633 References

634

635 1. Golden JW & Riddle DL (1984) The Caenorhabditis elegans dauer larva: developmental
636 effects of pheromone, food, and temperature. *Dev Biol* 102(2):368-378.
637 2. Swanson MM & Riddle DL (1981) Critical periods in the development of the
638 Caenorhabditis elegans dauer larva. *Dev Biol* 84(1):27-40.
639 3. Hu PJ (2007) Dauer. *WormBook*:1-19.
640 4. Karp X (2018) Working with dauer larvae. *WormBook* 2018:1-19.
641 5. Fielenbach N & Antebi A (2008) C. elegans dauer formation and the molecular basis of
642 plasticity. *Genes Dev* 22(16):2149-2165.
643 6. Burnell AM, Houthoofd K, O'Hanlon K, & Vanfleteren JR (2005) Alternate metabolism
644 during the dauer stage of the nematode Caenorhabditis elegans. *Exp Gerontol*
645 40(11):850-856.
646 7. Rashid S, Wong C, & Roy R (2021) Developmental plasticity and the response to nutrient
647 stress in Caenorhabditis elegans. *Dev Biol* 475:265-276.
648 8. Cohen SM, Wrobel CJJ, Prakash SJ, Schroeder FC, & Sternberg PW (2022) Formation
649 and function of dauer ascarosides in the nematodes Caenorhabditis briggsae and
650 Caenorhabditis elegans. *G3 (Bethesda)* 12(3).
651 9. Braendle C, Milloz J, & Felix MA (2008) Mechanisms and evolution of environmental
652 responses in Caenorhabditis elegans. *Curr Top Dev Biol* 80:171-207.
653 10. Diaz SA & Viney M (2015) The evolution of plasticity of dauer larva developmental arrest
654 in the nematode Caenorhabditis elegans. *Ecol Evol* 5(6):1343-1353.
655 11. Ewald CY, Landis JN, Porter Abate J, Murphy CT, & Blackwell TK (2015) Dauer-
656 independent insulin/IGF-1-signalling implicates collagen remodelling in longevity. *Nature*
657 519(7541):97-101.

658 12. Harvey SC, Shorto A, & Viney ME (2008) Quantitative genetic analysis of life-history traits
659 of Caenorhabditis elegans in stressful environments. *BMC Evol Biol* 8:15.
660 13. Zhu J & Thompson CB (2019) Metabolic regulation of cell growth and proliferation. *Nat*
661 *Rev Mol Cell Biol* 20(7):436-450.
662 14. Altan-Bonnet G & Mukherjee R (2019) Cytokine-mediated communication: a quantitative
663 appraisal of immune complexity. *Nat Rev Immunol* 19(4):205-217.
664 15. Douglas A, Stevens B, & Lynch L (2023) Interleukin-17 as a key player in
665 neuroimmunometabolism. *Nat Metab* 5(7):1088-1100.
666 16. Mills KHG (2022) IL-17 and IL-17-producing cells in protection versus pathology. *Nat Rev*
667 *Immunol*.
668 17. Li X, Bechara R, Zhao J, McGeachy MJ, & Gaffen SL (2019) IL-17 receptor-based
669 signaling and implications for disease. *Nat Immunol* 20(12):1594-1602.
670 18. Hall PA & Lane DP (1997) Tumor suppressors: a developing role for p53? *Curr Biol*
671 7(3):R144-147.
672 19. Jain AK & Barton MC (2018) p53: emerging roles in stem cells, development and beyond.
673 *Development* 145(8).
674 20. Levine AJ (2020) p53: 800 million years of evolution and 40 years of discovery. *Nat Rev*
675 *Cancer* 20(8):471-480.
676 21. Rutkowski R, Hofmann K, & Gartner A (2010) Phylogeny and function of the invertebrate
677 p53 superfamily. *Cold Spring Harb Perspect Biol* 2(7):a001131.
678 22. Pfister NT & Prives C (2017) Transcriptional Regulation by Wild-Type and Cancer-Related
679 Mutant Forms of p53. *Cold Spring Harb Perspect Med* 7(2).
680 23. Lu WJ, Amatruda JF, & Abrams JM (2009) p53 ancestry: gazing through an evolutionary
681 lens. *Nat Rev Cancer* 9(10):758-762.

682 24. Bowen ME, Mulligan AS, Sorayya A, & Attardi LD (2021) Puma- and Caspase9-mediated
683 apoptosis is dispensable for p53-driven neural crest-based developmental defects. *Cell*
684 *Death Differ* 28(7):2083-2094.
685 25. Van Nostrand JL & Attardi LD (2014) Guilty as CHARGED: p53's expanding role in
686 disease. *Cell Cycle* 13(24):3798-3807.
687 26. Chen C*, et al.* (2017) IL-17 is a neuromodulator of Caenorhabditis elegans sensory
688 responses. *Nature* 542(7639):43-48.
689 27. Flynn SM*, et al.* (2020) MALT-1 mediates IL-17 neural signaling to regulate C. elegans
690 behavior, immunity and longevity. *Nat Commun* 11(1):2099.
691 28. Lillis M, Zaccardi NJ, & Heiman MG (2022) Axon-dendrite and apical-basolateral sorting
692 in a single neuron. *Genetics* 221(1).
693 29. Golden JW & Riddle DL (1984) A pheromone-induced developmental switch in
694 Caenorhabditis elegans: Temperature-sensitive mutants reveal a wild-type temperature-
695 dependent process. *Proc Natl Acad Sci U S A* 81(3):819-823.
696 30. Thomas JH, Birnby DA, & Vowels JJ (1993) Evidence for parallel processing of sensory
697 information controlling dauer formation in Caenorhabditis elegans. *Genetics* 134(4):1105-
698 1117.
699 31. Vowels JJ & Thomas JH (1992) Genetic analysis of chemosensory control of dauer
700 formation in Caenorhabditis elegans. *Genetics* 130(1):105-123.
701 32. Ailion M & Thomas JH (2003) Isolation and characterization of high-temperature-induced
702 Dauer formation mutants in Caenorhabditis elegans. *Genetics* 165(1):127-144.
703 33. Li W & Ou G (2016) The application of somatic CRISPR-Cas9 to conditional genome
704 editing in Caenorhabditis elegans. *Genesis* 54(4):170-181.
705 34. Paix A*, et al.* (2014) Scalable and versatile genome editing using linear DNAs with
706 microhomology to Cas9 Sites in Caenorhabditis elegans. *Genetics* 198(4):1347-1356.

707 35. Xu S (2015) The application of CRISPR-Cas9 genome editing in Caenorhabditis elegans.
708 *J Genet Genomics* 42(8):413-421.
709 36. Holt SJ (2006) Staying alive in adversity: transcriptome dynamics in the stress-resistant
710 dauer larva. *Funct Integr Genomics* 6(4):285-299.
711 37. Cohen SM, Sun JJ, Schroeder FC, & Sternberg PW (2021) Transcriptional Response to
712 a Dauer-Inducing Ascaroside Cocktail in Late L1 in C. elegans. *MicroPubl Biol* 2021.
713 38. Wang J & Kim SK (2003) Global analysis of dauer gene expression in Caenorhabditis
714 elegans. *Development* 130(8):1621-1634.
715 39. Wirick MJ*, et al.* (2021) daf-16/FOXO blocks adult cell fate in Caenorhabditis elegans
716 dauer larvae via lin-41/TRIM71. *PLoS Genet* 17(11):e1009881.
717 40. Kyani-Rogers T*, et al.* (2022) Developmental history modulates adult olfactory behavioral
718 preferences via regulation of chemoreceptor expression in Caenorhabditiselegans.
719 *Genetics* 222(3).
720 41. Ow MC, Borziak K, Nichitean AM, Dorus S, & Hall SE (2018) Early experiences mediate
721 distinct adult gene expression and reproductive programs in Caenorhabditis elegans.
722 *PLoS Genet* 14(2):e1007219.
723 42. Motola DL*, et al.* (2006) Identification of ligands for DAF-12 that govern dauer formation
724 and reproduction in C. elegans. *Cell* 124(6):1209-1223.
725 43. Vowels JJ & Thomas JH (1994) Multiple chemosensory defects in daf-11 and daf-21
726 mutants of Caenorhabditis elegans. *Genetics* 138(2):303-316.
727 44. Lin K, Dorman JB, Rodan A, & Kenyon C (1997) daf-16: An HNF-3/forkhead family
728 member that can function to double the life-span of Caenorhabditis elegans. *Science*
729 278(5341):1319-1322.
730 45. Libina N, Berman JR, & Kenyon C (2003) Tissue-specific activities of C. elegans DAF-16
731 in the regulation of lifespan. *Cell* 115(4):489-502.

732 46. Lee SS, Kennedy S, Tolonen AC, & Ruvkun G (2003) DAF-16 target genes that control
733 C. elegans life-span and metabolism. *Science* 300(5619):644-647.
734 47. Kenyon C & Murphy CT (2006) Enrichment of regulatory motifs upstream of predicted
735 DAF-16 targets. *Nat Genet* 38(4):397-398; author reply 398.
736 48. da Graca LS*, et al.* (2004) DAF-5 is a Ski oncoprotein homolog that functions in a neuronal
737 TGF beta pathway to regulate C. elegans dauer development. *Development* 131(2):435-
738 446.
739 49. Gems D*, et al.* (1998) Two pleiotropic classes of daf-2 mutation affect larval arrest, adult
740 behavior, reproduction and longevity in Caenorhabditis elegans. *Genetics* 150(1):129-
741 155.
742 50. Zecic A & Braeckman BP (2020) DAF-16/FoxO in Caenorhabditis elegans and Its Role in
743 Metabolic Remodeling. *Cells* 9(1).
744 51. Oh SW*, et al.* (2005) JNK regulates lifespan in Caenorhabditis elegans by modulating
745 nuclear translocation of forkhead transcription factor/DAF-16. *Proc Natl Acad Sci U S A*
746 102(12):4494-4499.
747 52. Greer EL*, et al.* (2007) An AMPK-FOXO pathway mediates longevity induced by a novel
748 method of dietary restriction in C. elegans. *Curr Biol* 17(19):1646-1656.
749 53. Leiser SF, Begun A, & Kaeberlein M (2011) HIF-1 modulates longevity and healthspan in
750 a temperature-dependent manner. *Aging Cell* 10(2):318-326.
751 54. Perrin AJ*, et al.* (2013) Noncanonical control of C. elegans germline apoptosis by the
752 insulin/IGF-1 and Ras/MAPK signaling pathways. *Cell Death Differ* 20(1):97-107.
753 55. Gurkar AU*, et al.* (2018) Dysregulation of DAF-16/FOXO3A-mediated stress responses
754 accelerates oxidative DNA damage induced aging. *Redox Biol* 18:191-199.
755 56. Baruah A*, et al.* (2014) CEP-1, the Caenorhabditis elegans p53 homolog, mediates
756 opposing longevity outcomes in mitochondrial electron transport chain mutants. *PLoS*
757 *Genet* 10(2):e1004097.

758 57. Ewald CY, Castillo-Quan JI, & Blackwell TK (2018) Untangling Longevity, Dauer, and
759 Healthspan in Caenorhabditis elegans Insulin/IGF-1-Signalling. *Gerontology* 64(1):96-
760 104.
761 58. Derry WB, Putzke AP, & Rothman JH (2001) Caenorhabditis elegans p53: role in
762 apoptosis, meiosis, and stress resistance. *Science* 294(5542):591-595.
763 59. Schumacher B, Hofmann K, Boulton S, & Gartner A (2001) The C. elegans homolog of
764 the p53 tumor suppressor is required for DNA damage-induced apoptosis. *Curr Biol*
765 11(21):1722-1727.
766 60. Prives C (1998) Signaling to p53: breaking the MDM2-p53 circuit. *Cell* 95(1):5-8.
767 61. Schumacher B*, et al.* (2005) Translational repression of C. elegans p53 by GLD-1
768 regulates DNA damage-induced apoptosis. *Cell* 120(3):357-368.
769 62. Sendoel A, Kohler I, Fellmann C, Lowe SW, & Hengartner MO (2010) HIF-1 antagonizes
770 p53-mediated apoptosis through a secreted neuronal tyrosinase. *Nature* 465(7298):577-
771 583.
772 63. Gartner A, Boag PR, & Blackwell TK (2008) Germline survival and apoptosis.
773 *WormBook*:1-20.
774 64. Schumacher B*, et al.* (2005) C. elegans ced-13 can promote apoptosis and is induced in
775 response to DNA damage. *Cell Death Differ* 12(2):153-161.
776 65. Levi-Ferber M*, et al.* (2014) It's all in your mind: determining germ cell fate by neuronal
777 IRE-1 in C. elegans. *PLoS Genet* 10(10):e1004747.
778 66. Hicks T*, et al.* (2022) R-loop-induced irreparable DNA damage evades checkpoint
779 detection in the C. elegans germline. *Nucleic Acids Res* 50(14):8041-8059.
780 67. Greiss S, Schumacher B, Grandien K, Rothblatt J, & Gartner A (2008) Transcriptional
781 profiling in C. elegans suggests DNA damage dependent apoptosis as an ancient function
782 of the p53 family. *BMC Genomics* 9:334.

783 68. Schertel C & Conradt B (2007) C. elegans orthologs of components of the RB tumor
784 suppressor complex have distinct pro-apoptotic functions. *Development* 134(20):3691-
785 3701.
786 69. Arum O & Johnson TE (2007) Reduced expression of the Caenorhabditis elegans p53
787 ortholog cep-1 results in increased longevity. *J Gerontol A Biol Sci Med Sci* 62(9):951-
788 959.
789 70. Lee CC*, et al.* (2014) Mutation of a Nopp140 gene dao-5 alters rDNA transcription and
790 increases germ cell apoptosis in C. elegans. *Cell Death Dis* 5:e1158.
791 71. Sulston JE & Horvitz HR (1977) Post-embryonic cell lineages of the nematode,
792 Caenorhabditis elegans. *Dev Biol* 56(1):110-156.
793 72. Sternberg PW (2005) Vulval development. *WormBook*:1-28.
794 73. Horvitz HR & Sternberg PW (1982) Nematode postembryonic cell lineages. *J Nematol*
795 14(2):240-248.
796 74. Chisholm AD & Hardin J (2005) Epidermal morphogenesis. *WormBook*:1-22.
797 75. Herman MA (2006) Hermaphrodite cell-fate specification. *WormBook*:1-16.
798 76. Costa M, Weir M, Coulson A, Sulston J, & Kenyon C (1988) Posterior pattern formation in
799 C. elegans involves position-specific expression of a gene containing a homeobox. *Cell*
800 55(5):747-756.
801 77. Euling S & Ambros V (1996) Reversal of cell fate determination in Caenorhabditis elegans
802 vulval development. *Development* 122(8):2507-2515.
803 78. Braendle C & Felix MA (2008) Plasticity and errors of a robust developmental system in
804 different environments. *Dev Cell* 15(5):714-724.
805 79. Karp X & Greenwald I (2013) Control of cell-fate plasticity and maintenance of
806 multipotency by DAF-16/FoxO in quiescent Caenorhabditis elegans. *Proc Natl Acad Sci*
807 *U S A* 110(6):2181-2186.

808 80. Tenen CC & Greenwald I (2019) Cell Non-autonomous Function of daf-18/PTEN in the
809 Somatic Gonad Coordinates Somatic Gonad and Germline Development in C. elegans
810 Dauer Larvae. *Curr Biol* 29(6):1064-1072 e1068.
811 81. Hong Y, Roy R, & Ambros V (1998) Developmental regulation of a cyclin-dependent
812 kinase inhibitor controls postembryonic cell cycle progression in Caenorhabditis elegans.
813 *Development* 125(18):3585-3597.
814 82. Karp X & Ambros V (2012) Dauer larva quiescence alters the circuitry of microRNA
815 pathways regulating cell fate progression in C. elegans. *Development* 139(12):2177-2186.
816 83. O'Keeffe C & Greenwald I (2022) EGFR signal transduction is downregulated in C.
817 elegans vulval precursor cells during dauer diapause. *Development* 149(21).
818 84. Colella E, Li S, & Roy R (2016) Developmental and Cell Cycle Quiescence Is Mediated
819 by the Nuclear Hormone Receptor Coregulator DIN-1S in the Caenorhabditis elegans
820 Dauer Larva. *Genetics* 203(4):1763-1776.
821 85. Narbonne P & Roy R (2006) Inhibition of germline proliferation during C. elegans dauer
822 development requires PTEN, LKB1 and AMPK signalling. *Development* 133(4):611-619.
823 86. Wong C, Kadekar P, Jurczak E, & Roy R (2023) Germline stem cell integrity and
824 quiescence are controlled by an AMPK-dependent neuronal trafficking pathway. *PLoS*
825 *Genet* 19(4):e1010716.
826 87. Derry WB*, et al.* (2007) Regulation of developmental rate and germ cell proliferation in
827 Caenorhabditis elegans by the p53 gene network. *Cell Death Differ* 14(4):662-670.
828 88. Vousden KH & Ryan KM (2009) p53 and metabolism. *Nat Rev Cancer* 9(10):691-700.
829 89. Jones RG*, et al.* (2005) AMP-activated protein kinase induces a p53-dependent metabolic
830 checkpoint. *Mol Cell* 18(3):283-293.
831 90. Feng Y, Williams BG, Koumanov F, Wolstenholme AJ, & Holman GD (2013) FGT-1 is the
832 major glucose transporter in C. elegans and is central to aging pathways. *Biochem J*
833 456(2):219-229.

834 91. Schulz TJ*, et al.* (2007) Glucose restriction extends Caenorhabditis elegans life span by
835 inducing mitochondrial respiration and increasing oxidative stress. *Cell Metab* 6(4):280-
836 293.
837 92. Walker MD*, et al.* (2021) WormPaths: Caenorhabditis elegans metabolic pathway
838 annotation and visualization. *Genetics* 219(1).
839 93. Bargmann CI & Horvitz HR (1991) Control of larval development by chemosensory
840 neurons in Caenorhabditis elegans. *Science* 251(4998):1243-1246.
841 94. Das S, Min S, & Prahlad V (2021) Gene bookmarking by the heat shock transcription factor
842 programs the insulin-like signaling pathway. *Mol Cell* 81(23):4843-4860 e4848.
843 95. Das S*, et al.* (2020) Serotonin signaling by maternal neurons upon stress ensures progeny
844 survival. *Elife* 9.
845 96. Tatum MC*, et al.* (2015) Neuronal serotonin release triggers the heat shock response in
846 C. elegans in the absence of temperature increase. *Curr Biol* 25(2):163-174.
847 97. Ooi FK & Prahlad V (2017) Olfactory experience primes the heat shock transcription factor
848 HSF-1 to enhance the expression of molecular chaperones in C. elegans. *Sci Signal*
849 10(501).
850 98. Venkatesh H & Monje M (2017) Neuronal Activity in Ontogeny and Oncology. *Trends*
851 *Cancer* 3(2):89-112.
852 99. Curry RN & Glasgow SM (2021) The Role of Neurodevelopmental Pathways in Brain
853 Tumors. *Front Cell Dev Biol* 9:659055.
854
855

Figure 1

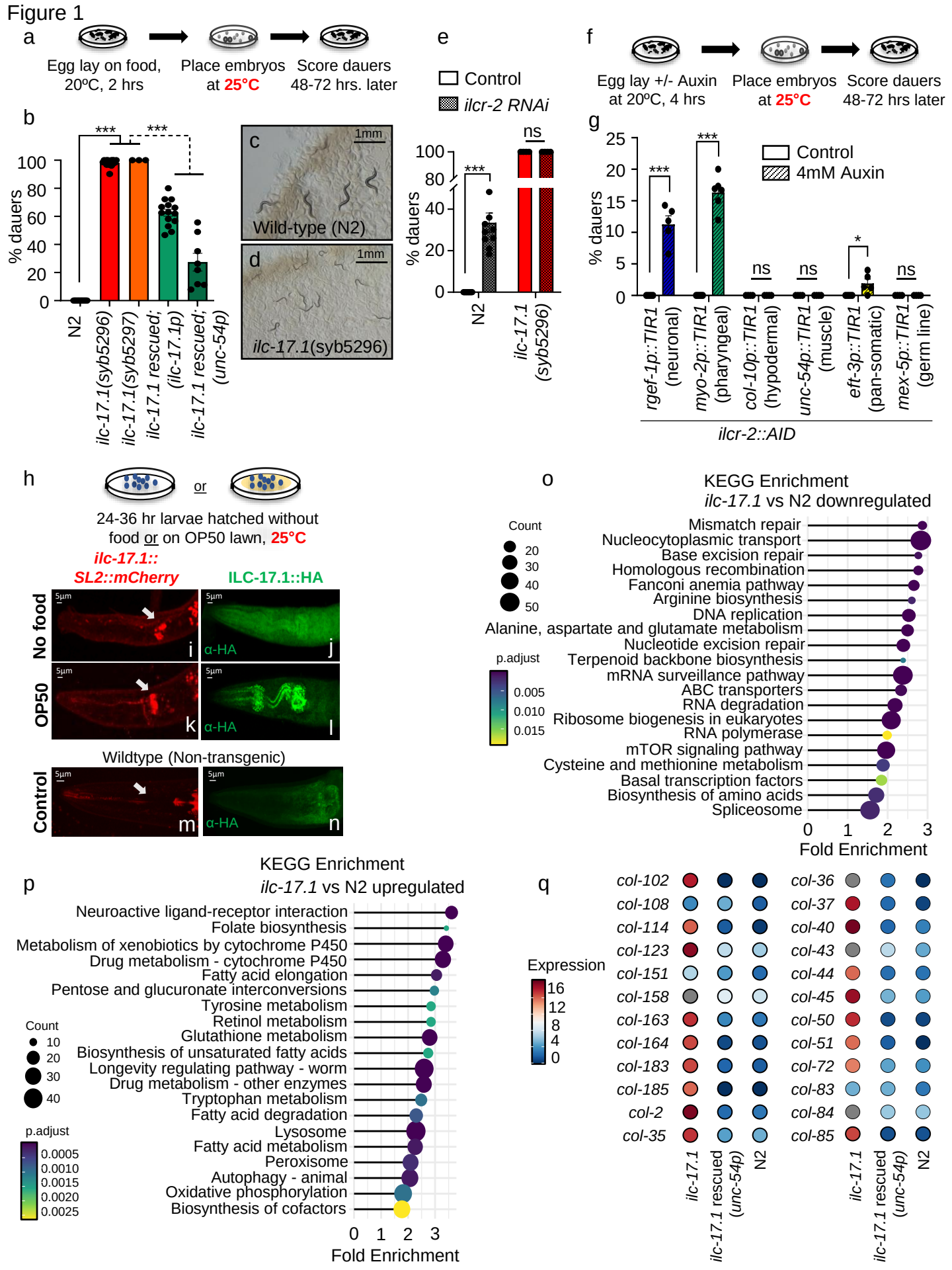
a
Egg lay on food, 20ºC, 2 hrs
Place embryos at 25°C
Score dauers 48-72 hrs. later
b
% dauers
N2
ilc-17.1(syb5296)
ilc-17.1(syb5297)
ilc-17.1 rescued; (ilc-17.1p)
ilc-17.1 rescued; (unc-54p)
c
1mm
Wild-type (N2)
d
1mm
ilc-17.1(syb5296)
e
Control
ilcr-2 RNAi
ns
% dauers
N2
ilc-17.1 (syb5296)
f
Egg lay +/- Auxin at 20ºC, 4 hrs
Place embryos at 25°C
Score dauers 48-72 hrs later
g
Control
4mM Auxin
% dauers
rgef-1p::TIR1 (neuronal)
myo-2p::TIR1 (pharyngeal)
col-10p::TIR1 (hypodermal)
unc-54p::TIR1 (muscle)
eft-3p::TIR1 (pan-somatic)
mex-5p::TIR1 (germ line)
ilcr-2::AID
h
or
24-36 hr larvae hatched without food or on OP50 lawn, 25°C
ilc-17.1:: SL2::mCherry
ILC-17.1::HA
No food
OP50
Wildtype (Non-transgenic)
Control
α-HA
o
KEGG Enrichment
ilc-17.1 vs N2 downregulated
Count
p.adjust
Mismatch repair
Nucleocytoplasmic transport
Base excision repair
Homologous recombination
Fanconi anemia pathway
Arginine biosynthesis
DNA replication
Alanine, aspartate and glutamate metabolism
Nucleotide excision repair
Terpenoid backbone biosynthesis
mRNA surveillance pathway
ABC transporters
RNA degradation
Ribosome biogenesis in eukaryotes
RNA polymerase
mTOR signaling pathway
Cysteine and methionine metabolism
Basal transcription factors
Biosynthesis of amino acids
Spliceosome
Fold Enrichment
p
KEGG Enrichment
ilc-17.1 vs N2 upregulated
Neuroactive ligand-receptor interaction
Folate biosynthesis
Metabolism of xenobiotics by cytochrome P450
Drug metabolism - cytochrome P450
Fatty acid elongation
Pentose and glucuronate interconversions
Tyrosine metabolism
Retinol metabolism
Glutathione metabolism
Biosynthesis of unsaturated fatty acids
Longevity regulating pathway - worm
Drug metabolism - other enzymes
Tryptophan metabolism
Fatty acid degradation
Lysosome
Fatty acid metabolism
Peroxisome
Autophagy - animal
Oxidative phosphorylation
Biosynthesis of cofactors
Fold Enrichment
q
Expression
col-102
col-108
col-114
col-123
col-151
col-158
col-163
col-164
col-183
col-185
col-2
col-35
col-36
col-37
col-40
col-43
col-44
col-45
col-50
col-51
col-72
col-83
col-84
col-85
ilc-17.1
ilc-17.1 rescued (unc-54p)
N2

Figure 2

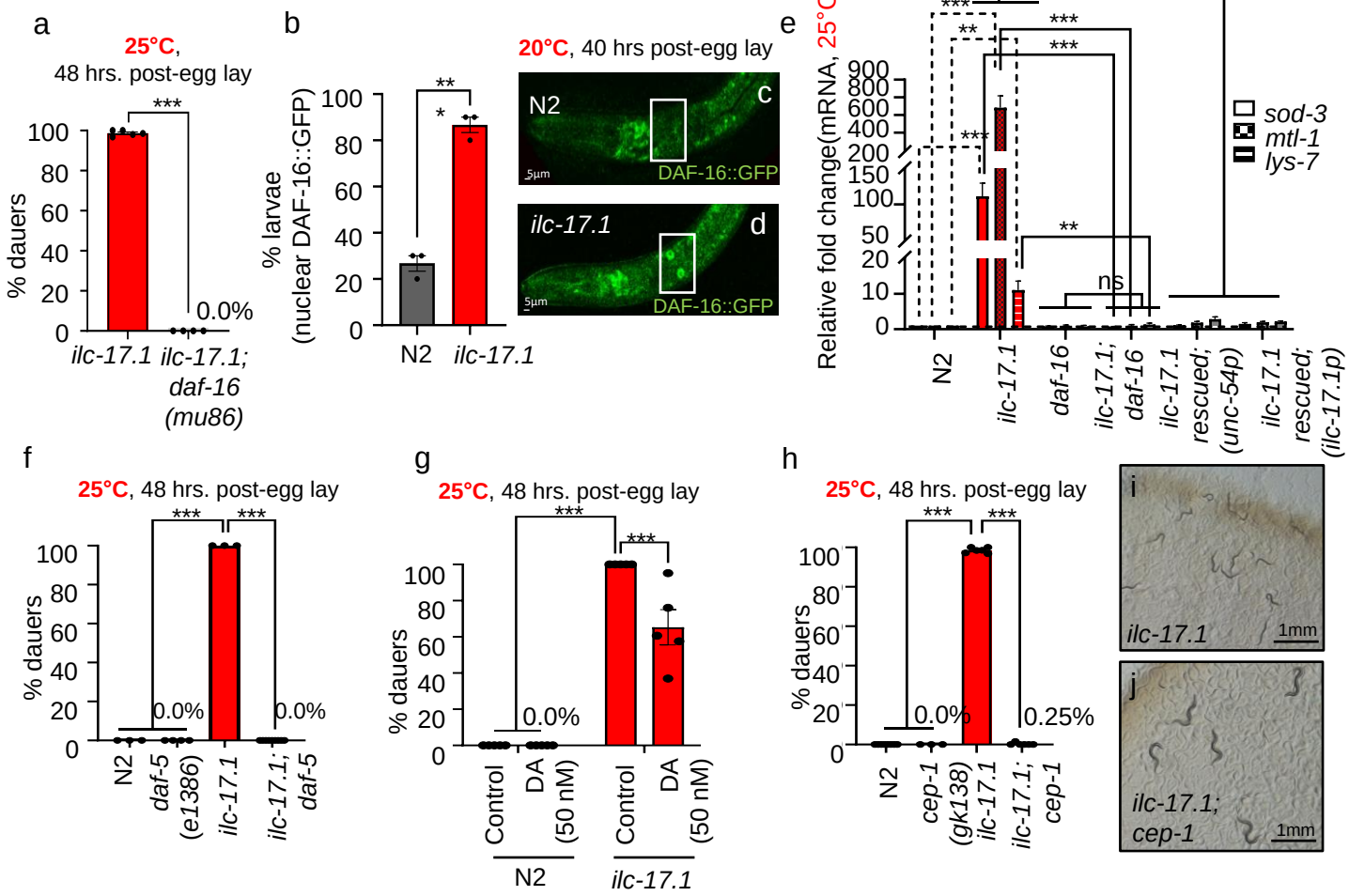
a
25°C,
48 hrs. post-egg lay
% dauers
***
0.0%
ilc-17.1
ilc-17.1; daf-16 (mu86)
b
% larvae (nuclear DAF-16::GFP)
**
*
N2
ilc-17.1
20°C, 40 hrs post-egg lay
N2
c
DAF-16::GFP
ilc-17.1
d
DAF-16::GFP
e
Relative fold change(mRNA, 25°C)
sod-3
mtl-1
lys-7
ns
N2
ilc-17.1
daf-16
ilc-17.1; daf-16
ilc-17.1 rescued; (unc-54p)
ilc-17.1 rescued; (ilc-17.1p)
f
25°C, 48 hrs. post-egg lay
% dauers
0.0%
N2
daf-5 (e1386)
ilc-17.1
ilc-17.1; daf-5
g
25°C, 48 hrs. post-egg lay
% dauers
0.0%
Control
DA (50 nM)
N2
ilc-17.1
h
25°C, 48 hrs. post-egg lay
% dauers
0.0%
0.25%
N2
cep-1 (gk138)
ilc-17.1
ilc-17.1; cep-1
i
ilc-17.1
1mm
j
ilc-17.1; cep-1
1mm

Figure 3

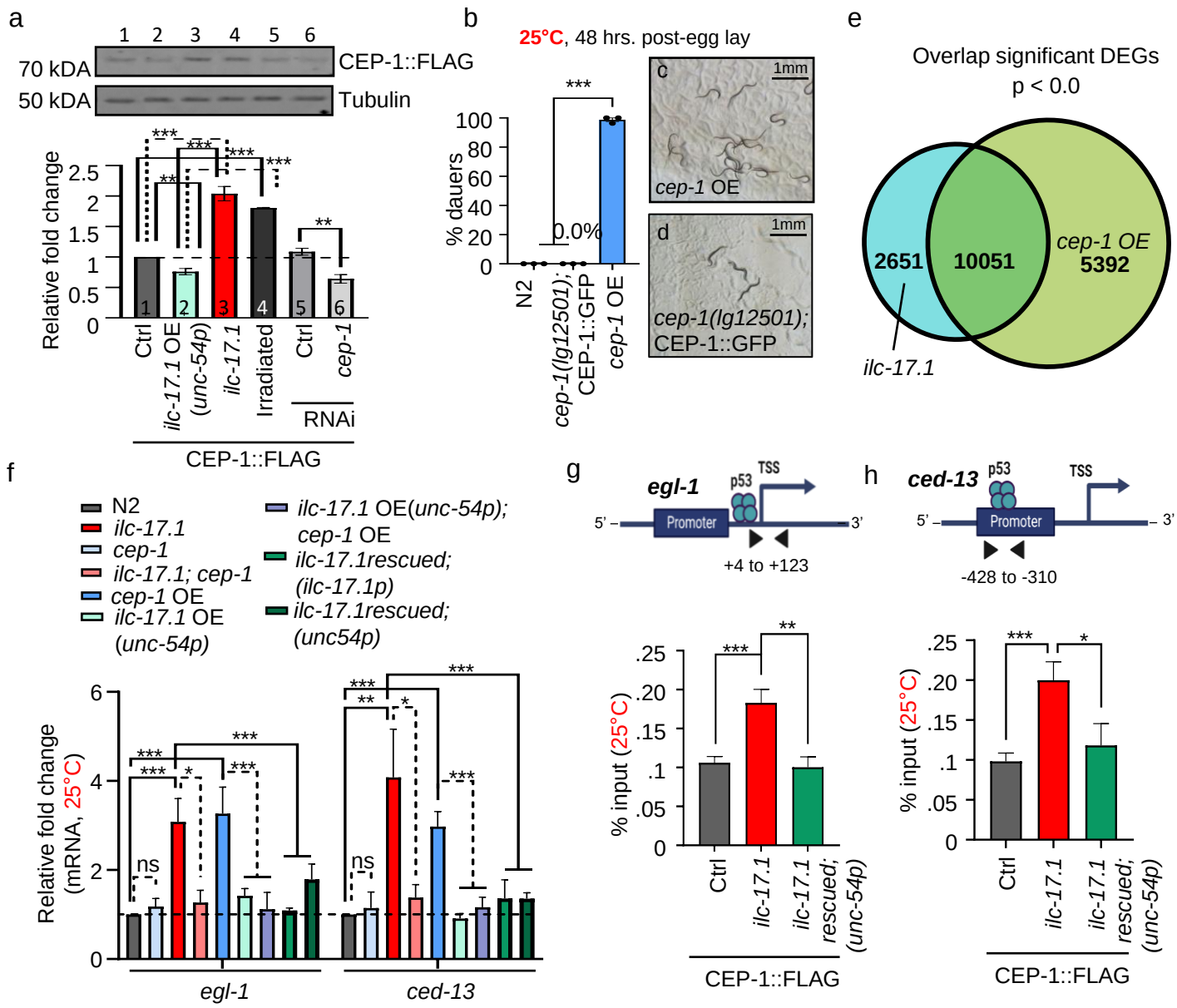
a
1 2 3 4 5 6
70 kDA
CEP-1::FLAG
50 kDA
Tubulin
Relative fold change
Ctrl
ilc-17.1 OE (unc-54p)
ilc-17.1
Irradiated
Ctrl
cep-1
RNAi
CEP-1::FLAG
b
25°C, 48 hrs. post-egg lay
% dauers
0.0%
N2
cep-1(lg12501); CEP-1::GFP
cep-1 OE
c
1mm
cep-1 OE
d
1mm
cep-1(lg12501); CEP-1::GFP
e
Overlap significant DEGs
p < 0.0
2651
10051
cep-1 OE
5392
ilc-17.1
f
N2
ilc-17.1
cep-1
ilc-17.1; cep-1
cep-1 OE
ilc-17.1 OE (unc-54p)
ilc-17.1 OE(unc-54p); cep-1 OE
ilc-17.1rescued; (ilc-17.1p)
ilc-17.1rescued; (unc54p)
Relative fold change (mRNA, 25°C)
ns
egl-1
ced-13
g
egl-1
p53
TSS
Promoter
5'
3'
+4 to +123
% input (25°C)
Ctrl
ilc-17.1
ilc-17.1 rescued; (unc-54p)
CEP-1::FLAG
h
ced-13
p53
TSS
Promoter
5'
3'
-428 to -310
% input (25°C)
Ctrl
ilc-17.1
ilc-17.1 rescued; (unc-54p)
CEP-1::FLAG

Figure 4

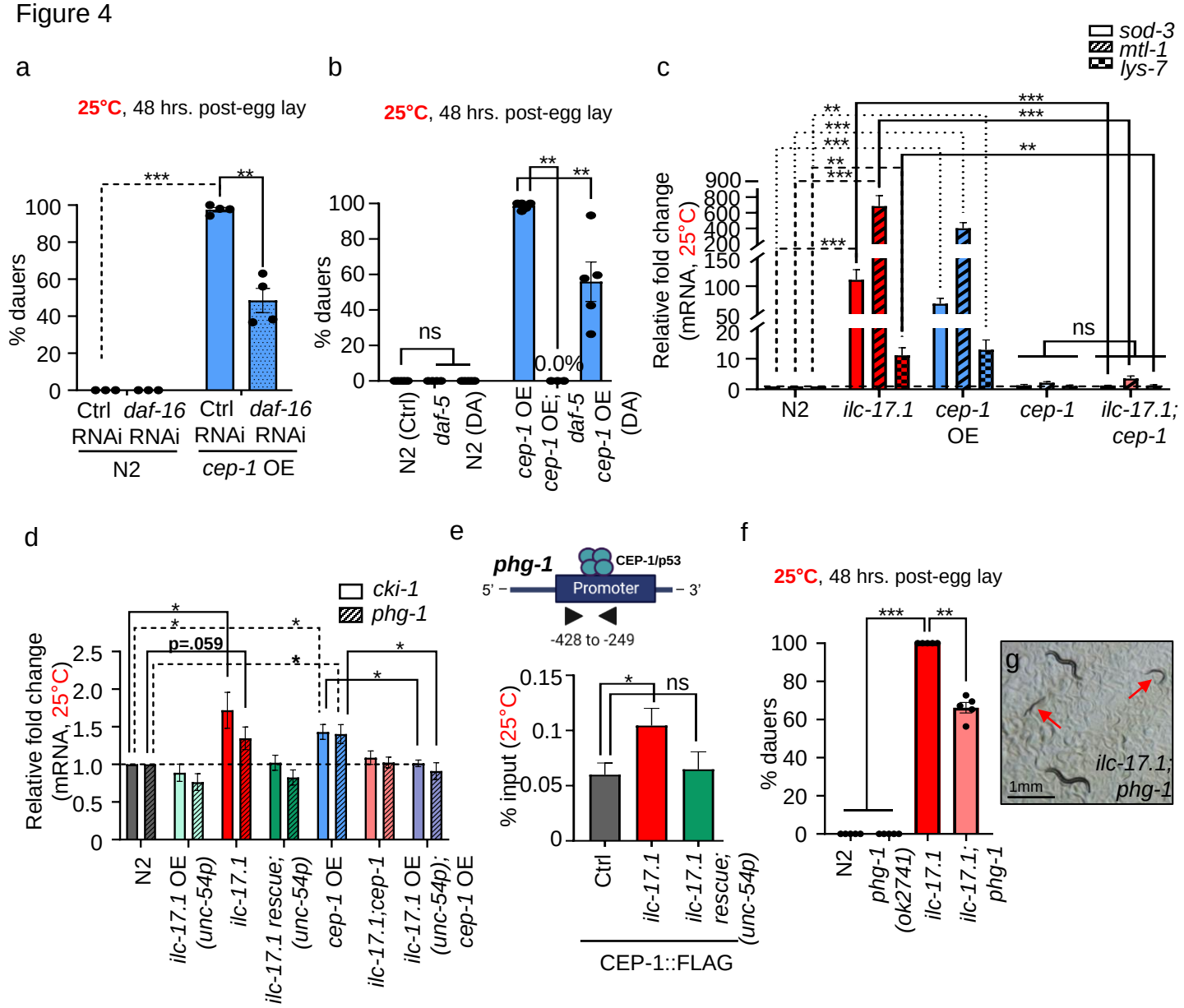
a
25°C, 48 hrs. post-egg lay
% dauers
Ctrl RNAi
daf-16 RNAi
Ctrl RNAi
daf-16 RNAi
N2
cep-1 OE
b
25°C, 48 hrs. post-egg lay
% dauers
ns
0.0%
N2 (Ctrl)
daf-5
N2 (DA)
cep-1 OE
cep-1 OE; daf-5
cep-1 OE (DA)
c
sod-3
mtl-1
lys-7
Relative fold change (mRNA, 25°C)
N2
ilc-17.1
cep-1 OE
cep-1
ilc-17.1; cep-1
ns
d
cki-1
phg-1
p=.059
Relative fold change (mRNA, 25°C)
N2
ilc-17.1 OE (unc-54p)
ilc-17.1
ilc-17.1 rescue; (unc-54p)
cep-1 OE
ilc-17.1;cep-1
ilc-17.1 OE (unc-54p); cep-1 OE
e
phg-1
CEP-1/p53
Promoter
5'
3'
-428 to -249
% input (25°C)
ns
Ctrl
ilc-17.1
ilc-17.1 rescue; (unc-54p)
CEP-1::FLAG
f
25°C, 48 hrs. post-egg lay
% dauers
N2
phg-1 (ok2741)
ilc-17.1
ilc-17.1; phg-1
g
ilc-17.1; phg-1
1mm

Figure 5

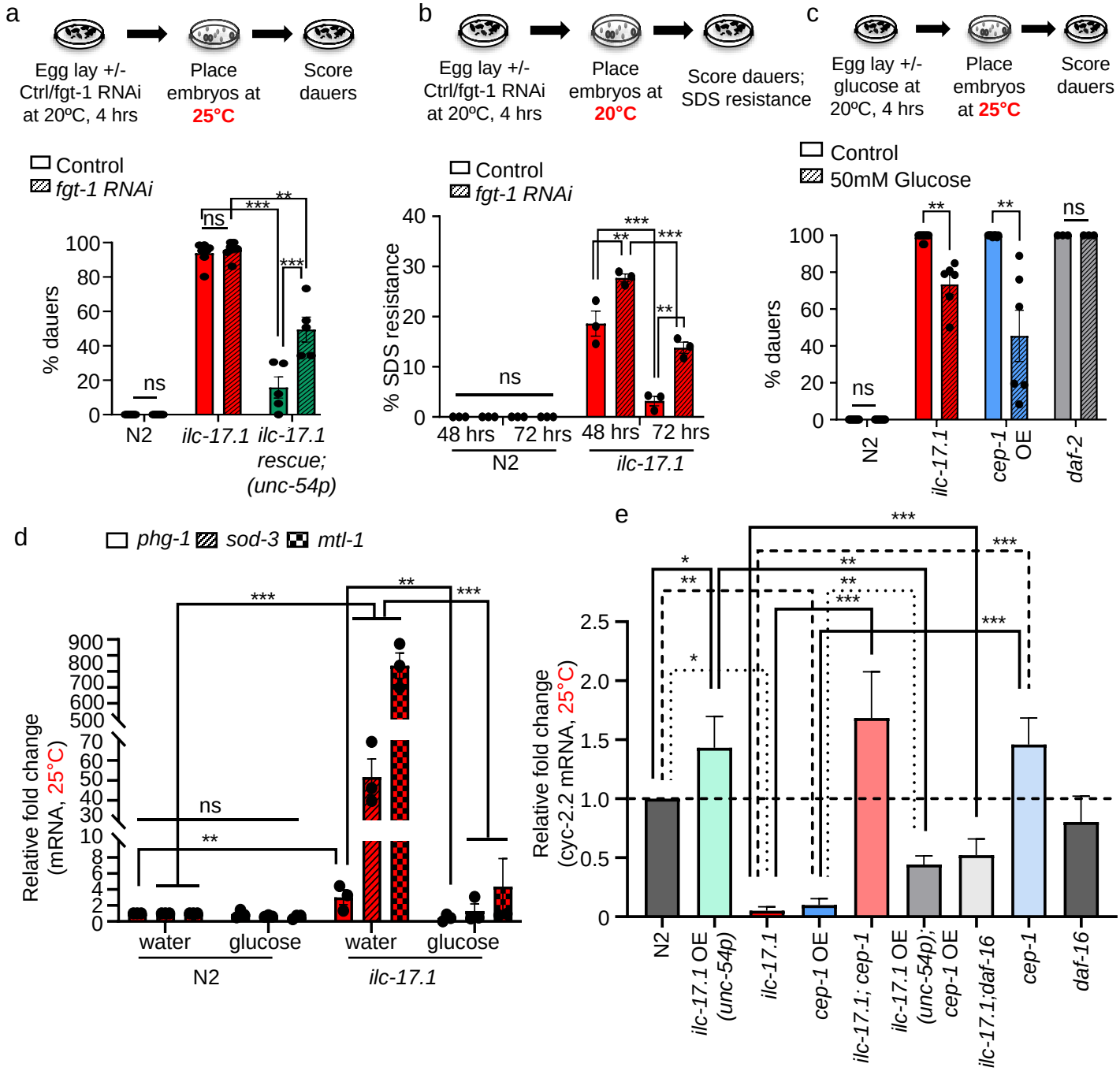
a
Egg lay +/- Ctrl/fgt-1 RNAi at 20ºC, 4 hrs
Place embryos at 25°C
Score dauers
b
Egg lay +/- Ctrl/fgt-1 RNAi at 20ºC, 4 hrs
Place embryos at 20°C
Score dauers; SDS resistance
c
Egg lay +/- glucose at 20ºC, 4 hrs
Place embryos at 25°C
Score dauers
Control
fgt-1 RNAi
% dauers
N2
ilc-17.1
ilc-17.1 rescue; (unc-54p)
% SDS resistance
48 hrs
72 hrs
50mM Glucose
cep-1 OE
daf-2
d
phg-1
sod-3
mtl-1
Relative fold change (mRNA, 25°C)
water
glucose
e
Relative fold change (cyc-2.2 mRNA, 25°C)
ilc-17.1 OE (unc-54p)
cep-1 OE
ilc-17.1; cep-1
ilc-17.1 OE (unc-54p); cep-1 OE
ilc-17.1;daf-16
cep-1
daf-16

Figure 6

a

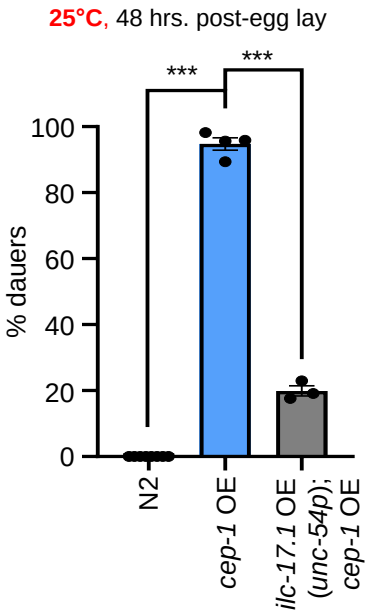

b

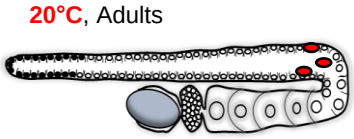
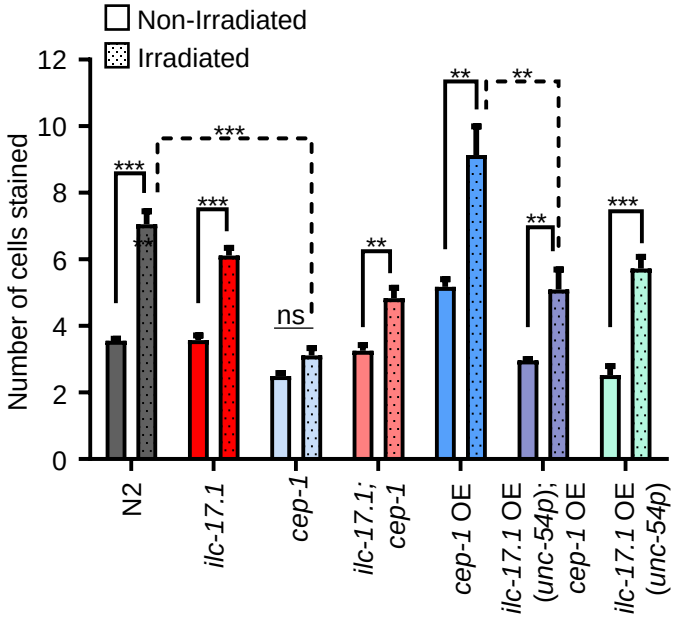
apoptotic nuclei: Acridine Orange staining